Dynamic Stability Enhancement of Power System Using Fuzzy Logic Based Power System Stabilizer

Kamalesh Chandra Rout

Department of Electrical Engineering
National Institute of Technology,Rourkela
Rourkela-769008, Odisha, INDIA
May 2011

Dynamic Stability Enhancement of Power System Using Fuzzy Logic Based Power System Stabilizer

A thesis submitted in partial fulfillment of the requirements for the degree of

Master of Technology by Research

in

Electrical Engineering

by

Kamalesh Chandra Rout

(Roll-608EE309)

Under the Guidance of

Prof. P.C. PANDA

Department of Electrical Engineering

National Institute of Technology,Rourkela

Rourkela-769008, Odisha, INDIA

May 2011

Department of Electrical Engineering

National Institute of Technology, Rourkela

C E R T I F I C A T E

This is to certify that the thesis entitled ***"Dynamic Stability Enhancement of Power System Using Fuzzy Logic Based Power System Stabilizer"*** *by* ***Mr. Kamalesh Chandra Rout****, submitted to the National Institute of Technology, Rourkela (Deemed University) for the award of Master of Technology by Research in Electrical Engineering, is a record of bonafide research work carried out by him in the Department of Electrical Engineering , under my supervision. I believe that this thesis fulfills part of the requirements for the award of degree of Master of Technology by Research.The results embodied in the thesis have not been submitted for the award of any other degree elsewhere.*

Place:Rourkela

Date:

Prof. P.C. PANDA

DEDICATED TO MY BELOVED PARENTS WHO LED ME TO THIS ACCOMPLISHMENT

Acknowledgements

Words are inadequate to express the overwhelming sense of gratitude and humble regards to my supervisor Prof. P.C. Panda, Professor, Department of Electrical Engineering for his constant motivation, support, expert guidance, constant supervision and constructive suggestion for the submission of my progress report of thesis work ”Dynamic Stability Enhancement of Power System Using Fuzzy Logic Based Power System Stabilizer”.

I express my gratitude to Prof. Bidyadhar Subudhi, Head of the Department, for his help and support during my study. I am thankful for the opportunity to be a member of National institute of technology of Electrical Engineering Department. I express my gratitude to the members of Masters Scrutiny Committee, Professors K.B. Mohanty, K.K. Mohapatra and G.K. Panda for their advice and care.

I also thank all the teaching and non-teaching staff for their nice cooperation to the students.

I would like to thank all whose direct and indirect support helped me completing my thesis in time.

This report would have been impossible if not for the perpetual moral support from my family members, and my friends. I would like to thank them all.

Kamalesh Chandra Rout

Rourkela, May 2011

Abstract

Power systems are subjected to low frequency disturbances that might cause loss of synchronism and an eventual breakdown of entire system. The oscillations, which are typically in the frequency range of 0.2 to 3.0 Hz, might be excited by the disturbances in the system or, in some cases, might even build up spontaneously. These oscillations limit the power transmission capability of a network and, sometimes, even cause a loss of synchronism and an eventual breakdown of the entire system. For this purpose, Power system stabilizers (PSS) are used to generate supplementary control signals for the excitation system in order to damp these low frequency power system oscillations.

The use of power system stabilizers has become very common in operation of large electric power systems. The conventional PSS which uses lead-lag compensation, where gain settings designed for specific operating conditions, is giving poor performance under different loading conditions. The constantly changing nature of power system makes the design of CPSS a difficult task. Therefore, it is very difficult to design a stabilizer that could present good performance in all operating points of electric power systems. To overcome the drawback of conventional power system stabilizer (CPSS), many techniques such as fuzzy logic, genetic algorithm, neural network etc. have been proposed in the literature.

In an attempt to cover a wide range of operating conditions, Fuzzy logic based technique has been suggested as a possible solution to overcome the above problem, thereby using this technique complex system mathematical model can be avoided, while giving good performance under different operating conditions. Fuzzy Logic has the features of simple concept, easy implementation, and computationally efficient. The fuzzy logic based power system stabilizer model is evaluated on a single machine infinite bus power system, and then the performance of Conventional power system stabilizer (CPSS) and Fuzzy logic based Power system stabilizer (FLPSS) are compared. Results presented in the thesis demonstrate that the fuzzy logic based power system stabilizer design gives better performance than the Conventional Power system stabilizer.

Contents

List of Abbreviations

Abbreviation	Description
AVR	Automatic Voltage Regulator
AEA	Adaptive Evolutionary Algorithm
ANFIS	Adaptive Neuro-Fuzzy Inference System
CPSS	Conventional Power System Stabilizer
COS	Centre of Sum
FLPSS	Fuzzy Logic Power System Stabilizer
FL	Fuzzy Logic
FRMG	Fuzzy Reference Model Generator
GN	Generalized Neuron
GA	Genetic Algorithm
LFO	Low Frequency Oscillation
MF	Membership Function
MOM	Mean of Maxima
MISO	Multi Input Single Output
MRAC	Model Reference Adaptive Controller
NN	Neural Network
PSS	Power System Stabilizer
PI	Proportional Integral
PID	Proportional Integral Derivative
RFLPSS	Robust Fuzzy Logic Power System Stabilizer
RNNC	Recurrent Neural Network Controller
SMIB	Single Machine Infinite Bus
STR	Self Tuning Regulator

List of Figures

List of Tables

Chapter 1

INTRODUCTION

1.1 Power System Stability

Power system stability is the tendency of a power system to develop restoring forces equal to or greater than the disturbing forces to maintain the state of equilibrium. Since power systems rely on synchronous machines for generation of electrical power, a necessary condition for satisfactory system operation is that all synchronous machines remain in synchronism. This aspect of stability is influenced by the dynamics of generator rotor angles and power-angle relationships.

The power system is a dynamic system. The electrical power systems today are no longer operated as isolated systems, but as interconnected systems which may include thousands of electric elements and be spread over vast geographical areas. There are many advantages of interconnected power systems

- Provide large blocks of power and increase reliability of the system.
- Reduce the number of machines which are required both for operation at peak load and required as spinning reserve to take care of a sudden change of load.
- Provide economical source of power to consumers.

On the other hand there are disadvantages of using interconnected power systems. The interconnecting ties between neighboring power systems are relatively weak when compared to the connections within the system. It easily leads to low frequency inter oscillation. Many of the early instances of oscillation instability occur at low frequencies when interconnections are made. Power system stability can be classified into three categories.

1. Steady-state stability :

   Steady-state stability analysis is the study of power system and its generators in strictly steady state conditions and trying to answer the question of what is the maximum possible generator load that can be transmitted without loss of synchronism of any one generator. The maximum power is called the steady-state stability limit.

   For an n- machine power system the active power fed in by the i_{th} generator is defined by the (1.1).

$$P_i = \frac{U_{pi}^2}{Z_{ii}} \sin \alpha_{ii} + U_{pi} \sum_{\substack{j=1 \\ i \neq i}}^{n} \frac{U_{pi}}{Z_{ij}} \sin(\delta_i - \delta_j - \alpha_{ij}) \qquad (1.1)$$

   where U_{pi} is the magnitude of the internal voltage (the voltage behind synchronous reactance) of the generator (line to line voltage);

   $Z_{ii}(\frac{\pi}{2} - \alpha_{ii})$ is the driving point impedance; $Z_{ij}(\frac{\pi}{2} - \alpha_{ij})$ is the transfer impedance between machines $i$and$j$; δ_i is the phase angle lead (load angle) of the i_{th} generator with respect to the reference phasor and P_i is the electrical three phase power of the generator.

   Assuming that the load angles of all other machines are constant, the steady-state stability limit can be predicted from equation (1.1).

   A common problem is the insidious nature of the oscillatory instability. Power flow over a tie line may be increased to supply remote load with no noticeable problems until the stability limit is reached. A slight increase in power flow beyond this limit results in oscillations in which amplitude increases quickly with no need for any system fault. At best system non-linearity limit oscillation amplitude. At worst, the oscillation amplitudes reach levels at which protective relays trip lines and generation, and this in turn causes partial or total system collapse [43].

2. Transient stability :

   Transient stability is the ability of the power system to maintain synchronism when subjected to a sudden and large disturbance within a small time such as a fault on transmission facilities, loss of generation or loss of a large load [4].

   The system response to such disturbances involves large excursions of generator rotor angles, power flows, bus voltages etc.

   It is a fast phenomenon usually occurring within 1 second for a generator close to the cause of disturbance such as 3-phase to ground fault, line to ground fault etc.

3. Dynamic Stability :

   A system is said to be dynamically stable if the oscillations do not acquire more than certain amplitude and die out quickly. Dynamic stability is a concept used in the study of transient conditions in power systems. Any electrical disturbances in a power system will cause electromechanical transient processes. Besides the electrical transient phenomena produced, the power balance of the generating units is always disturbed, and thereby mechanical oscillations of machine rotors follow the disturbance [38].

   To describe the transient phenomena, the well-known swing equation of the synchronous generators, derived from the torque equation for synchronous machine, can be used:

$$T_{wi}\frac{d^2\delta_i}{dt^2} = P_{Mi} - D_i\frac{d}{dt}\delta_i - P_{Ei} \tag{1.2}$$

where T_{wi} is the impulse moment of the rotor of the generating unit,D_i is the damping coefficient (representing the mechanical as well as the electrical damping effect), δ_i is the phase angle (load angle), P_{Mi} is the turbine power applied to rotor and P_{Ei} is the electrical power output from the stator.

1.1.1 Types of Oscillations

The disturbances occurring in power system include electromechanical oscillations of electrical generators. These oscillations are also called power swings and these must be effectively damped to maintain the system stability. Electromechanical oscillations can be classified in four main categories.

1. Local oscillations: - Between a unit and rest of generating station and between the later and rest of power system. Their frequency typically ranges from 0.2 Hz to 2.5 Hz.

2. Interplant oscillations: - Between two electrically close generating plants. Frequency can vary from 1 Hz to 2 Hz.

3. Interarea oscillations: - Between two major groups of generating plants. Frequencies are typically in the range of 0.2 Hz to 0.8 Hz, generally called low frequency oscillations.

4. Global oscillations: - Characterized by a common in phase oscillations of all generators as found on an isolated system. The frequency of such global mode is typically under 0.2 Hz.

1.1.2 Low Frequency Oscillations

Low frequency oscillations (LFOs) are generator rotor angle oscillations having a frequency between 0.1 Hz to 3.0 Hz and are defined by how they are created or where they are located in the power system. The use of high gain exciters, poorly turned generation excitation, HVDC converters may create LFOs with negative damping; this is a small-signal stability problem. The mitigation of these oscillations is commonly performed with ”supplementary stabilizing signals” and the networks used to generate these signals have come to be known as ”power system stabilizer” networks. LFOs include local plant modes, control modes, torsional modes induced by the interaction between the mechanical and electrical modes of a turbine-generator system, and inter-area modes, which may be caused by either high gain exciters or heavy power transfers across weak tie lines.

Low frequency oscillations can be created by small disturbances in the system, such as changes in the load, and are normally analyzed through the small-signal stability (linear response) of the power system. These small disturbances lead to a steady increase or decrease in generator rotor angle caused by the lack of synchronizing torque, or to rotor oscillations of increasing amplitude due to a lack of sufficient damping torque. The most typical instability is the lack of a sufficient damping torque on the rotor's low frequency oscillations.

1.2 Literature Survey

1.2.1 Power System Stabilizer (PSS)

A. Dysko, W.E. Leithead and J. O'Reilly [18] have described a step-by-step coordinated design procedure for power system stabilizers (PSSs) and automatic voltage regulators (AVRs) in a strongly coupled system. The proposed coordinated PSS/AVR design procedure is established within a frequency-domain framework. Chow and Sanchez-Gasca [13] proposes a power system stabilizer using pole placement technique and this work is carried by Yu and Li [55] for a nine bus system. G Guralla, R Padhi and I Sen [23] have proposed a method of designing fixed parameter decentralized power system stabilizers (PSS) for interconnected multi machine power systems. Here Heffron - Philips model is used to decide the structure of the PSS compensator and tune its parameters at each machine in the multi machine environment. A. Chatterjee, S.P. Ghosal, and V. Mukherjee [9] have described a comparative transient performance of single-input conventional power system stabilizer (CPSS) and dual-input power system stabilizer (PSS), namely PSS4B. An experience of dynamic instability [50] has analyzed in this paper. The method of analysis was to determine stability by the calculation of the Eigen values of the system. Explanation is provided [6] regarding small signal stability, high impedance transmission lines, line loading, and high gain, fast acting excitation systems. An experience in assigning PSS projects [14] has discussed in an under graduate control design course to provide students with a challenging design problem using three different techniques (root-locus, frequency-domain, state-space) and to expose them to power system engineering. A generalized neuron (GN) that requires much smaller training data and shorter training time has developed and by taking benefit of these characteristics of the GN, a new power system stabilizer is proposed [10]. Wah-Chun Chan, Yuan-Yih Hsu [8] presents a technique for designing an optimal variable structure stabilizer for improving the dynamic stability of power systems by increasing the damping torque of the synchronous machine in the system. De Mello [15] has explored the phenomenon of stability of synchronous machines under small perturbations by examining the case of single machine connected to an infinite bus through external reactance. The design of PSS for single machine connected to an infinite bus has been described [19] using fast output sampling feedback. A step-up transformer is used to set up a modified Heffron-Philips (ModHP) model. The PSS design based on this model utilizes signals available within the generating station [22]. An augmented PSS

[35] is described which extends the performance capabilities into the weak tie-line case. E.V Larsen and D.A Swann [31] have presented in their 3 paper titled 'Applying power system stabilizer - I, II, III' the history of power system stabilizer and its role in a power system. Practical means have been developed using Eigen value [16] analysis techniques to guide the selection process. An extended quasi-steady-state model [52] has presented that includes low-frequency interarea oscillations which can be used effectively for the design of power system stabilizers. Wlfred Watson and Gerald Manchur [53] has suggested that the use of high speed excitation for generator static excitation systems results in decreased damping, which has detrimental impact on steady state stability, i.e. it may be lost even at normal full load operation.

1.2.2 PID (Proportional-Integral-Derivative) Controller

Radman and Smaili [40] have proposed the PID based power system stabilizer and Wu and Hsu [12] have proposed the self tuning PID power system stabilizer for a multi machine power system. M. Dobrescu, I. Kamwa [17] in their paper has described a PID (proportional-integral-derivative) type FLPSS with adjustable gains added outside in order to keep a simple structure. In order to validate the FLPSS, it has been compared with two reference stabilizers; the IEEE PSS4B and IEEE PSS2B form the IEEE STD 421.5. A. Jalilvand, R. Aghmasheh and E. Khalkhali in their paper [27] have described the tuning of Proportional Integral Derivative power system stabilizers (PID-PSS) using Artificial intelligence (AI) technique.

1.2.3 Genetic Algorithm

G.H. Hwang [26] have described a design of fuzzy power system stabilizer (FPSS) using an adaptive evolutionary algorithm (AEA). AEA consists of Genetic Algorithm (GA) for a global search capability and evolution strategy (ES) for a local search in an adaptive manner. AEA is used to optimize the membership functions and scaling factors of FPSS. A.S. Al-Hinai and S.M. Al-Hinai [2] have used Genetic Algorithm for a proper design of a power system stabilizer. A Babaei, S.E. Razavi, S.A. Kamali, A. Gholami [5] have used a modified Genetic Algorithm for suitable design of stabilizer.

1.2.4 Fuzzy Logic Controller

Lin [32] proposed a fuzzy logic power system stabilizer which could shorten the tuning process of fuzzy rules and membership functions. The proposed PSS has two stages, first stage develops a proportional derivative type PSS, in the second stage it is transformed into FLPSS. Roosta, A.R, [44] have described three proposed types of fuzzy control algorithms and tested in the case of single machine connected to the network for various types of disturbance. S.A. Taher has proposed a novel robust fuzzy logic power system stabilizer (RFLPSS). Here to provide robustness, additional signal namely speed is used as inputs to RFLPSS enabling appropriate gain adjustments [48]. M.L. Kothari, T. Kumar [29] have presented a new approach for designing a fuzzy logic power system stabilizer such that it improves both transient and dynamic stabilities. Here they have considered FLPSS based on 3, 5 and 7 MFs of Gaussian shape. T. Hussein [25] has described an indirect variable-structure adaptive fuzzy controller as a power system stabilizer (IDVSFPSS) to damp inter-area modes of oscillation following disturbances in power systems. S.K. Yee and J.V. Milanovic [54] have proposed a decentralized fuzzy logic controller using a systematic analytical method based on a performance index. F. Rashidi [42] has described a fuzzy sliding mode controller in which a simple fuzzy inference mechanism is used to estimate the upper bound of uncertainties. Kamalasadan, S and Swann, G [28] have proposed a fuzzy model reference adaptive controller uses a fuzzy reference model generator (FRMG) in parallel with the model reference adaptive controller (MRAC). N. Gupta and S.K. Jain [21] have described the performance of single machine infinite bus system with fuzzy power system stabilizer. Here the generator is represented by the standard K-coefficients as second order systems and the performance is investigated for Trapezoidal, Triangular Gaussian membership functions of input and output variables. M. Ramirez, O.P. Malik [41] have described a simplified fuzzy logic controller (SFLC) with a significantly reduced set of fuzzy rules, small number of tuning parameters and simple control algorithm and structure. T. Hussein [47] has presented a robust adaptive fuzzy controller as a power system stabilizer (RFPSS) to damp inter-area modes of oscillation following disturbances in power systems. Matsuki et al. [36] described the process of determination of optimal fuzzy control parameters by trial and error. R. Gupya, D.K. Sambariya, R. Gunjan [20] have discussed a study of fuzzy logic power system stabilizer (PSS) for stability enhancement of a multi machine power system. H.M. Behbehani [7] have used fuzzy logic principles to develop supervisory power system stabilizers (SPSS) to enhance damping of inter-area oscillations to improve stability and reliability of power system subjected to disturbances. N.Nallathambi presents a study of fuzzy logic power system stabilizer for stability enhancement of a two-area four machine system [37]. Park and Lee [39] proposed a self organizing power system stabilizer where the rules are generated automatically and rule base updated online by self organizing procedure. Lu J. [33] proposed a fuzzy logic based adaptive power system stabilizer. A. Singh has described the design of a fuzzy logic based controller to counter the small-signal oscillatory instability in power systems [45]. K.L. Al-Olimat [3] has presented a self tuning regulator (STR) with multi identification models and a minimum variance controller that utilizes fuzzy logic switching. Taliyat et al. [49] proposed an augmented fuzzy PSS. Hussein et al. [24] proposed self tuning power system stabilizer in which two tuning parameters are introduced to tune fuzzy logic PSS. Abdelazim and Malik [1] proposed a self learning fuzzy logic power system stabilizer.

1.2.5 Neuro-Fuzzy Inference System

M. F. Othman, M. Mahfouf and D.A. Linkens, have described the design procedure for a fuzzy logic based power system stabilizer (FLPSS) and adaptive neuro-fuzzy inference system (ANFIS) and investigates their robustness for a multi-machine power system. Speed deviation of a machine and its derivative are chosen as the input signals to the FLPSS [34]. Vani, M.U, Raju, G.S and Prasad, K.R.L [51] in their paper have presented a step-by-step design methodology of an adaptive Neuro-Fuzzy inference system and optimization methods based automatic voltage regulator and power system stabilizer. Chun-Jung Chen [11] has presented an adaptive power system stabilizer (PSS) which consists of a recurrent neural network controller (RNNC) and a compensator to damp the oscillations of power system. The function of RNNC is to supply an adaptive control signal to the exciter or governor, which can damp most of the power system's oscillations. Sumina D. [46] have presented the usage of neural network (NN) based excitation control on single machine infinite bus. The proposed feed forward neural network integrates a voltage regulator and a power system stabilizer.

1.3 Problem Statement

Some of the earliest power system stability problems included spontaneous power system oscillations at low frequencies. These low frequency oscillations (LFOs) are related to the small signal stability of a power system and are detrimental to the goals of maximum power transfer and power system security. Once the solution of using damper windings on the generator rotors and turbines to control these oscillations was found to be satisfactory, the stability problem was thereby disregarded for some time. However, as power systems began to be operated closer to their stability limits, the weakness of a synchronizing torque among the generators was recognized as a major cause of system instability. Automatic voltage regulators (AVRs) helped to improve the steady-state stability of the power systems. But with the creation of large, interconnected power systems, another concern was the transfer of large amounts of power across extremely long transmission lines. The addition of a supplementary controller into the control loop, such as the introduction of conventional power system stabilizers (CPSSs) to the AVRs on the generators, provides the means to reduce the inhibiting effects of low frequency oscillations. The conventional power system stabilizers work well at the particular network configuration and steady state conditions for which they were designed. Once conditions change the performance degrades.

The conventional power system stabilizer such as lead-lag, proportional integral (PI) power system stabilizer, proportional integral derivative (PID) power system stabilizer operates at a certain point. So the disadvantage of this type of stabilizer is they cannot operate under different disturbances.

This can be overcome by a PSS design based on Fuzzy logic technique.

1.4 Solution Methodology

To overcome the drawbacks of conventional power system stabilizer (CPSS), numerous techniques have been proposed in the literature. In this thesis work, the conventional PSS's effect on the system damping is then compared with a fuzzy logic based PSS while applied to a single machine infinite bus (SMIB) power system. For the conventional design state space representation is used here.

1.5 Objectives of the Work

The objectives of the project are

- To study the nature of power system stability, excitation system, automatic voltage regulator for synchronous generator and power system stabilizer.

- To develop a fuzzy logic based power system stabilizer which will make the system quickly stable when fault occurred in the transmission line.
- By using simulation to validate fuzzy logic based power system stabilizer and its performance is compared with conventional power system stabilizer and without power system stabilizer.

1.6 Contributions of the Thesis

Chapter 1 :

Presents the introduction to power system stability, low frequency oscillations, literature survey, and objective of the work and chapter wise contribution of the thesis.

Chapter 2 :

Presents the modelling of power system and formation of the state space matrix of the single machine infinite bus (SMIB) system.

Chapter 3 :

Presents a frequency response method for the design of a conventional power system stabilizer (CPSS) in the frequency domain.

Chapter 4 :

Presents briefly the fuzzy logic control theory, need for implementing fuzzy controller. It also describes fuzzy logic based PSS.

Chapter 5 :

Presents results and discussions for without excitation system, with excitation system only, with conventional PSS, with fuzzy logic based PSS and a comparison between conventional PSS and fuzzy logic based PSS.

Chapter 6 :

Presents conclusion and suggestions for future work.

Chapter 2

MODELLING OF POWER SYSTEM

2.1 Introduction

For stability assessment of power system adequate mathematical models describing the system are needed. The models must be computationally efficient and be able to represent the essential dynamics of the power system. The mathematical model for small signal analysis of synchronous machine, excitation system and the lead-lag power system stabilizer are briefly reviewed.

2.2 Single Machine Infinite Bus (SMIB) Model

The performance of a synchronous machine connected to a large system through transmission lines has shown in Figure 2.1. The synchronous machine is vital for power system operation. The general system configuration of synchronous machine connected to infinite bus through transmission network can be represented as the Thevenin's equivalent circuit.

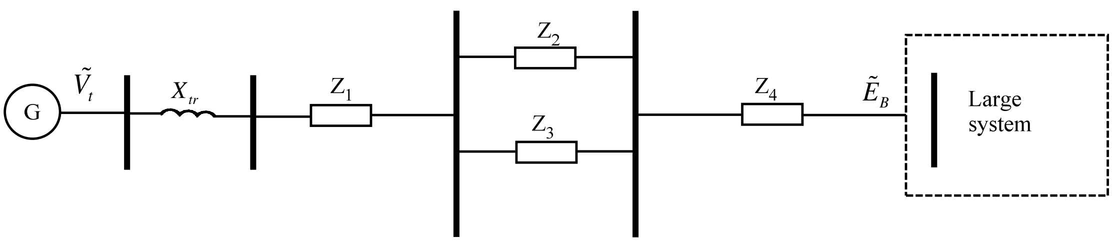

Figure 2.1: General Configuration of SMIB

At first the synchronous machine will be represented by the classical model. Then, the model details will be increased to account for the effects of the dynamics of the field circuit and the excitation system. The block diagram representation and torque-angle relationships will be used to analyze the system-stability characteristics. The block diagram representation and torque-angle relationships will be used to analyze the system-stability characteristics.

For the purpose of analysis, the system of Figure 2.1 may be reduced to the form of Figure 2.2.

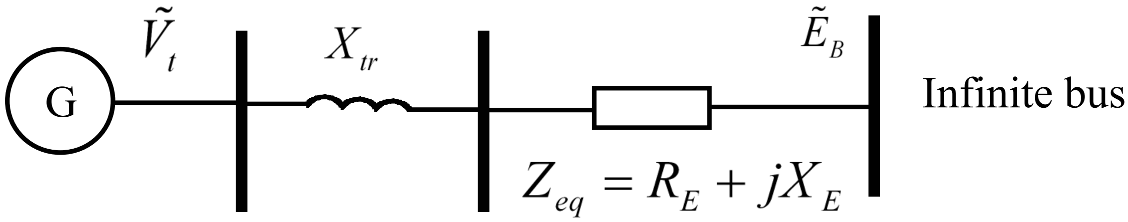

Figure 2.2: Equivalent Circuit of SMIB

2.2.1 Classical Model Representation of the Generator

The classical model representation of the generator [30] and with all the resistances neglected, the system representation is shown in Figure 2.3.

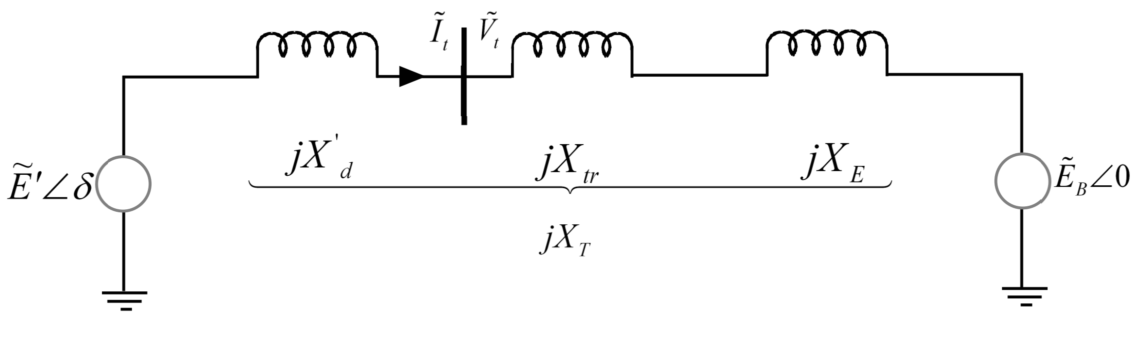

Figure 2.3: Classical model of the synchronous generator

In Figure 2.3, $\tilde{E}'$ is the voltage behind X'_d, which is the direct axis transient reactance of the generator. The magnitude of $\tilde{E}'$ is assume to remain constant at the pre-disturbance value. Let δ be the angle by which $\tilde{E}'$ leads the infinite bus voltage $\tilde{E}_B$.

The complex power behind X_d' is given by

$$S = P + jQ' = \tilde{E}'\tilde{I}_t^* = \frac{E' E_B \sin\delta}{X_T} + j\frac{E'(E' - E_B\cos\delta)}{X_T} \tag{2.1}$$

The equations of motion in per unit are

$$P\Delta\omega_r = \frac{1}{2H}\left[\Delta T_m - K_s\Delta\delta - K_D\Delta\omega_r\right] \tag{2.2}$$

$$P\Delta\delta = \omega_0\Delta\omega_r \tag{2.3}$$

Writing equations (2.2) and (2.3) in the vector-matrix form, we obtain

$$\frac{d}{dt}\begin{bmatrix}\Delta\omega_r\\ \Delta\delta\end{bmatrix} = \begin{bmatrix}-\frac{K_D}{2H} & -\frac{K_s}{2H}\\ \omega_0 & 0\end{bmatrix}\begin{bmatrix}\Delta\omega_r\\ \Delta\delta\end{bmatrix} + \begin{bmatrix}\frac{1}{2H}\\ 0\end{bmatrix}\Delta T_m \tag{2.4}$$

where $\Delta\omega_r$ is the per unit angular speed deviation of the rotor
H is the per unit inertia constant
T_m is the applied mechanical torque
K_D is the damping torque coefficient
δ is the rotor angle in electrical radians
ω_0 is the rotor speed in rad/sec
K_s is the synchronizing torque coefficient
The synchronizing torque coefficient K_s is given by

$$K_s = \frac{E' E_B}{X_T}\cos\delta_0 \tag{2.5}$$

This is the state-space representation of the system in the form $\dot{x} = Ax + Bu$. The elements of the state matrix A are seen to be dependent on the system parameters H,K_D, X_T and the initial operating condition represented by the values of $\tilde{E}'$ and δ_0. Vector b is also dependent on H.

Therefore, the undamped natural frequency is

$$\omega_n = \sqrt{K_s \frac{\omega_0}{2H}} \tag{2.6}$$

$$\zeta = \frac{1}{2}\frac{K_D}{2H\omega_n} = \frac{1}{2}\frac{K_D}{\sqrt{K_s 2H\omega_0}} \tag{2.7}$$

As the synchronizing torque coefficient K_s increases, the natural frequency increases and the damping ratio decreases. An increase in damping torque coefficient K_D increases the damping ratio, whereas an increase in inertia constant decreases both ω_n and ζ.

The phasor diagram of the relative positions of machine quantities is shown in Figure 2.4. As the rotor oscillates during a disturbance, δ changes.

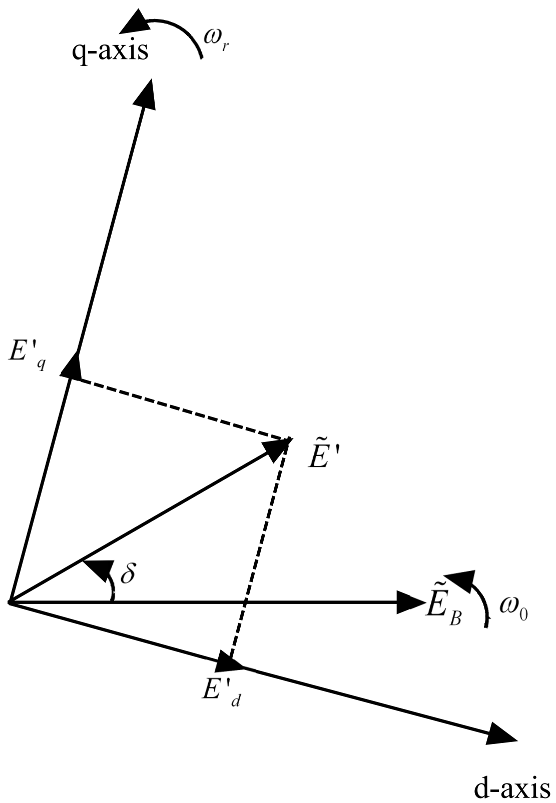

Figure 2.4: Phasor diagram of machine quantities

2.3 Effects of Synchronous Machine Field Circuit Dynamics

Now we consider the system performance including the effect of field flux variations. Then we will develop the state-space model of the system by first reducing the synchronous machine equations to an appropriate form and then combining them with the network equations.

As in the case of the classical generator model, the linearised equations of motion are

$$\frac{d}{dt}\Delta\omega_r = \frac{1}{2H}(\Delta T_m - \Delta T_e - K_D\Delta\omega_r) \tag{2.8}$$

$$\frac{d}{dt}\Delta\delta = \omega_0\Delta\omega_r \tag{2.9}$$

$$\frac{d}{dt}\Delta\delta = \omega_0\Delta\omega_r \tag{2.10}$$

where ΔT_e is the electrical (air-gap) torque. In this case, the rotor angle δ is the angle (in electrical radians) by which the q-axis leads the reference $\tilde{E}_B$. The phasor diagram shown in Figure 2.5 shows the relative position of synchronous machine variables. The rotor angle is given by

$$\delta = \delta_t + \delta_i \tag{2.11}$$

In Figure 2.5 δ_t is the angle by which the terminal voltage phasor $\tilde{V}_t$ leads the reference $\tilde{E}_B$ and the steady state value of δ_i is given by

$$\delta_i = a\tan\left(\frac{X_q I_t\cos\varphi - R_a I_t\sin\varphi}{V_t + R_a I_t\cos\varphi + X_q I_t\sin\varphi}\right) \tag{2.12}$$

where V_t and I_t are terminal voltage and current
φ is the power factor angle
R_a is the armature resistance per phase

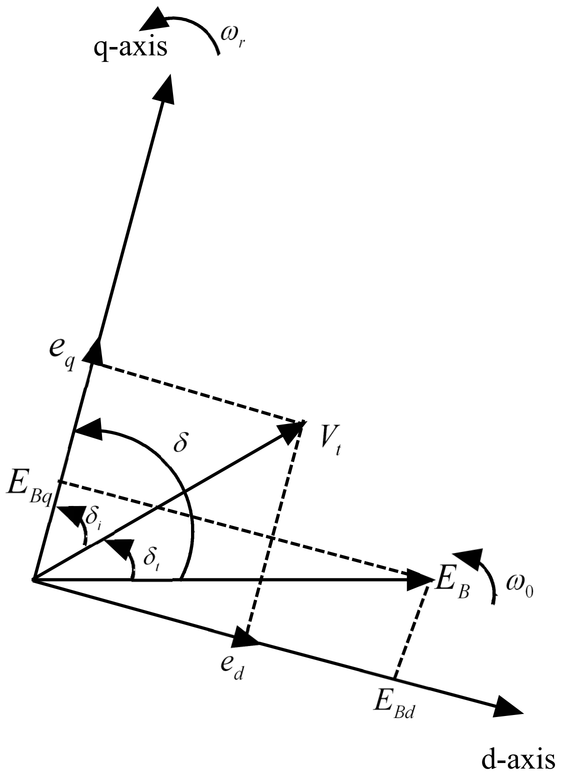

Figure 2.5: Phasor diagram of relative position of synchronous machine variables

X_q is the quadrature-axis synchronous reactance

The effect of field flux variations can be represented as

$$\frac{d}{dt}\Delta\psi_{fd} = \frac{\omega_0 R_{fd}}{L_{adu}}\Delta E_{fd} - \omega_0 R_{fd}\Delta i_{fd} \tag{2.13}$$

where $\Delta\psi_{fd}$ is the rotor circuit (field) flux linkage
R_{fd} is the rotor circuit resistance
L_{adu} is the unsaturated direct-axis manual inductance between stator and rotor windings
E_{fd} is the exciter output voltage
i_{fd} is the field circuit current

In order to develop the complete system equations in the state-space form ΔT_e and Δi_{fd} should be expressed in terms of the state variables as determined by the machine flux linkage equations and network equations. So we can write that

$$\Delta i_{fd} = \frac{1}{L_{fd}}\left(1 + m_2 L^{'}_{ads} - \frac{L^{'}_{ads}}{L_{fd}}\right)\Delta\psi_{fd} + \frac{1}{L_{fd}} m_1 L^{'}_{ads}\Delta\delta \qquad (2.14)$$

where

$$L^{'}_{ads} = \frac{L_{ads}L_{fd}}{L_{ads} + L_{fd}} \qquad (2.15)$$

$$m_1 = \frac{E_B(X_{Tq}\sin\delta_0 - R_T\cos\delta_0)}{D} \qquad (2.16)$$

$$m_2 = \frac{X_{Tq}}{D}\left(\frac{L_{ads}}{L_{ads} + L_{fd}}\right) \qquad (2.17)$$

$$R_T = R_a + R_E \qquad (2.18)$$

$$X_{Tq} = X_{tr} + X_E + (L_{aqs} + L_l) \qquad (2.19)$$

$$X_{Td} = X_{tr} + X_E + (L^{'}_{ads} + L_l) \qquad (2.20)$$

$$D = R_T^2 + X_{Tq}X_{Td} \qquad (2.21)$$

where X_{tr} is the reactance of the transformer
R_E is the Thevenin resistance of the network
X_E is the Thevenin reactance of the network
R_a is the armature resistance
L_l is the leakage inductance of the stator
L_{ads} is the saturated d-axis mutual inductance between stator and rotor windings
L_{aqs} is the saturated q-axis mutual inductance between stator and rotor windings
Also we can derive that

$$\Delta T_e = K_1\Delta\delta + K_2\Delta\psi_{fd} \qquad (2.22)$$

$$K_1 = n_1(\psi_{ad0} + L_{aqs} i_{d0}) - m_1(\psi_{aq0} + L'_{ads} i_{q0}) \tag{2.23}$$

$$K_2 = n_2(\psi_{ad0} + L_{aqs} i_{d0}) - m_2(\psi_{aq0} + L'_{aq0} i_{q0}) + \frac{L'_{ads}}{L_{fd}} i_{q0} \tag{2.24}$$

Here

$$n_1 = \frac{E_B(R_T \sin\delta_0 - X_{TD}\cos\delta_0)}{D} \tag{2.25}$$

$$n_2 = \frac{R_T}{D} \frac{L_{ads}}{(L_{ads} + L_{fd})} \tag{2.26}$$

$$i_{d0} = \frac{X_{Tq}\left[\psi_{fd0}\left(\frac{L_{ads}}{L_{ads}+L_{fd}}\right) - E_B\cos\delta_0\right] - R_T E_B \sin\delta_0}{D} \tag{2.27}$$

$$i_{q0} = \frac{R_T\left[\psi_{fd0}\left(\frac{L_{ads}}{L_{ads}+L_{fd}}\right) - E_B\cos\delta_0\right] - X_{Td} E_B \sin\delta_0}{D} \tag{2.28}$$

$$\psi_{ad0} = L'_{ads}\left(\frac{\psi_{fd0}}{L_{fd}} - i_{d0}\right) \tag{2.29}$$

$$\psi_{aq0} = -L_{aqs} i_{q0} \tag{2.30}$$

By substituting the expressions for Δi_{fd} and ΔT_e given by equations (2.13) and (2.21) into equations (2.8) and (2.12), the state-space representation of the system is obtained as follows:

$$\frac{d}{dt}\begin{bmatrix}\Delta\omega_r \\ \Delta\delta \\ \Delta\psi_{fd}\end{bmatrix} = \begin{bmatrix} a_{11} & a_{12} & a_{13} \\ a_{21} & 0 & 0 \\ 0 & a_{32} & a_{33}\end{bmatrix}\begin{bmatrix}\Delta\omega_r \\ \Delta\delta \\ \Delta\psi_{fd}\end{bmatrix} + \begin{bmatrix} b_{11} & 0 \\ 0 & 0 \\ 0 & b_{32}\end{bmatrix}\begin{bmatrix}\Delta T_m \\ \Delta E_{fd}\end{bmatrix} \tag{2.31}$$

where

$$a_{11} = -\frac{K_D}{2H} \tag{2.32}$$

$$a_{12} = -\frac{K_1}{2H} \tag{2.33}$$

$$a_{13} = -\frac{K_2}{2H} \tag{2.34}$$

$$a_{21} = \omega_0 = 2\Pi f_0 \tag{2.35}$$

$$a_{32} = -\frac{\omega_0 R_{fd}}{L_{fd}} m_1 L^{'}_{ads} \tag{2.36}$$

$$a_{33} = -\frac{\omega_0 R_{fd}}{L_{fd}} \left(m_2 L^{'}_{ads} + 1 - \frac{L^{'}_{ads}}{L_{fd}} \right) \tag{2.37}$$

$$b_{11} = \frac{1}{2H} \tag{2.38}$$

$$b_{32} = \frac{\omega_0 R_{fd}}{L_{adu}} \tag{2.39}$$

ΔT_m and ΔE_{fd} depend on prime mover and excitation controls. With constant mechanical input torque ΔT_m= 0; with constant exciter output voltage ΔE_{fd}= 0.

2.4 Representation of Saturation in Stability Studies

For stability studies the following assumptions are made in the representation of magnetic saturation.

- The leakage inductances are independent of saturation and only elements that saturate are the mutual inductances and .
- The leakage fluxes do not contribute to the iron saturation and the saturation is determined by the air-gap flux linkage.
- The saturation relationship between the resultant air-gap flux and the mmf under loaded conditions is the same as under no-load conditions.

- There is no magnetic coupling between the d- and q-axes.

2.5 Effects of Excitation system

The main objective of the excitation system is to control the field current of the synchronous machine. The field current is controlled so as to regulate the terminal voltage of the machine. As the field circuit time constant is high (of the order of a few seconds), fast control of the field current requires field forcing. Thus exciter should have a high ceiling voltage which enables it to operate transiently with voltage levels that are 3 to 4 times the normal. The rate of change of voltage should also be fast. Because of the high reliability required, unit exciter scheme is prevalent where each generating unit has its individual exciter. From the power system view point, the excitation system should contribute to effective control of voltage and enhancement of system stability. It should be capable of responding rapidly to a disturbance so as to enhance transient stability. In this dissertation, excitation control has been assumed for the purpose of analysis. Fundamentally, simplest excitation system consists of an exciter only. When the excitation system also performs the task of maintaining the terminal voltage of alternator constant, under varying load conditions, it incorporates voltage regulator also.

The functional block diagram of a typical control system for a large synchronous generator is shown in Figure 2.6. The following is a brief introduction of the various subsystems identified in the above Figure 2.6.

- Exciter: Provides dc power to the synchronous machine field winding, constituting the power angle of the excitation system.

- Regulator: processes and amplifies input control signal to a level and form appropriate for control of the exciter.

- Terminal voltage transducer and load compensator: senses generator terminal voltage, rectifies filters it to the dc quantity, compares it with a reference which represents the desired terminal voltage. In addition load compensation can be provided.

- Power system stabilizer: Provides an additional input signal to the regulator to damp power system oscillation. Some commonly used input signals are rotor speed deviation, accelerating power and frequency deviation.
- Limiter and protective circuits: These include a wide array of control and protective functions which ensure that the capability limits of exciter and generator are not exceeded. Common functions are field-current limiter, maximum excitation limiter, under excitation limiter etc.

Different types of excitation systems of synchronous generator are given below.

- DC excitation system: The system which utilize a direct current generator with a commutator as the source of excitation system power.

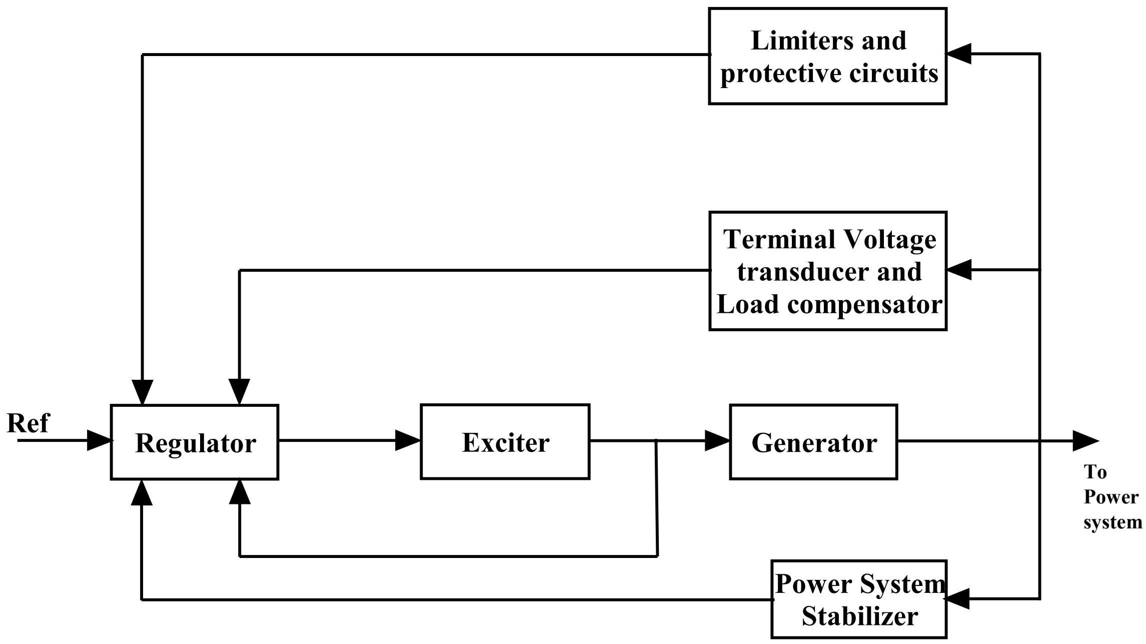

Figure 2.6: Block diagram of a synchronous generator excitation system

- AC excitation system: The system which uses an alternator and either stationary or rotating rectifiers to produce direct current needed for generator field.
- ST excitation system: The system in which excitation power is supplied through transformers and rectifiers.

The first two types of exciters are also called rotating exciters which are mounted on the same shaft as the generator and driven by the prime mover. The voltage regulator for DC excitation systems were based on rotating amplifier (amplidyne) or magnetic amplifiers. AC and static excitation systems invariably use electronic regulators which are fast acting and result in the phase control of the controlled rectifiers using thyristors. Static excitation system offers the ultimate response, which is virtually negligible, and ceiling voltage which are limited only by generator rotor design considerations. With the help of fast transient forcing of excitation and the boost of internal machine flux, the electrical output of the machine may be increased during the first swing compared to the results obtainable with a slow exciter. The static excitation system utilizes transformers to transform voltage to an appropriate level. Rectifiers, either controlled or non-controlled, provide the necessary direct current for generator field. The simplified model of a thyristor (static)

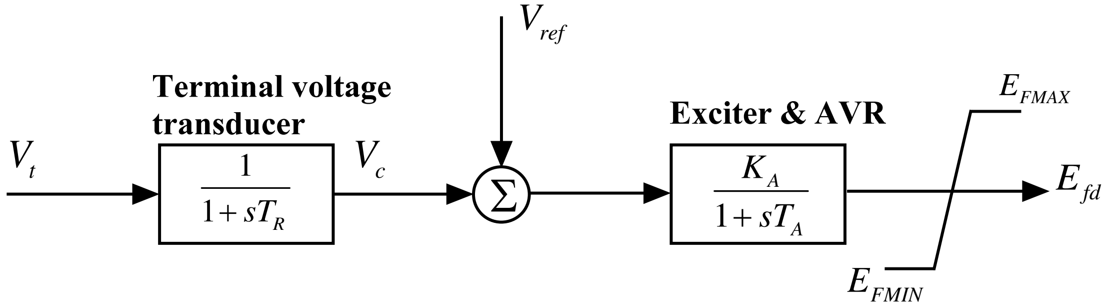

Figure 2.7: Block diagram of thyristor excitation system with AVR

excitation system is shown in Figure 2.7. A high exciter gain, without transient gain reduction or derivative feedback is used. Parameter T_R represents the terminal voltage transducer time constant. The only nonlinearity associated with this model is that due to the ceiling on the exciter output voltage represented by E_{FMAX} and E_{FMIN}. Due to small disturbances these limits are ignored so that E_{fd} is always within the limits and in Laplace domain can be given as

$$E_{fd} = \frac{K_A}{1 + sT_A}(V_{ref} - V_c) \tag{2.40}$$

Assuming that V_{ref} is constant during a short period after application of disturbance and by linearising equation (2.40), deviation of E_{fd} with respect to the steady state value is obtained as

$$\Delta E_{fd} = \frac{K_A}{1 + sT_A}(-\Delta V_c) \tag{2.41}$$

In the time domain the equation (2.41) can be written as

$$\frac{d}{dt}\Delta E_{fd} = -\frac{K_A}{T_A}\Delta V_c - \frac{1}{T_A}\Delta E_{fd} \tag{2.42}$$

From Figure 2.7 we can write that

$$\Delta V_c = \frac{1}{1 + sT_A}\Delta V_t \tag{2.43}$$

In the time domain equation (2.43) can be written as

$$\frac{d}{dt}\Delta V_c = \frac{1}{T_R}(\Delta V_t - \Delta V_c) \tag{2.44}$$

In order to obtain the state-space representation of the system, the state vector should be redefined. Equations (2.42) and (2.44) introduce two new state variables, namely ΔV_c and ΔE_{fd}. However ΔV_t is not a state variable and should be expressed in terms of other state variables. So we can write that

$$\Delta V_t = K_5 \Delta\delta + K_6 \Delta\psi_{fd} \tag{2.45}$$

where

$$K_5 = \frac{e_{d0}}{V_{t0}}\left[-R_a m_1 + L_1 n_1 + L_{aqs} n_1\right] + \frac{e_{q0}}{V_{t0}}\left[-R_a n_1 - L_1 m_1 - L_{ads} m_1\right] \tag{2.46}$$

$$K_6 = \frac{e_{d0}}{V_{t0}}\left[-R_a m_2 + L_1 n_2 + L_{aqs} n_2\right] + \frac{e_{q0}}{V_{t0}}\left[-R_a n_2 - L_1 m_2 + L^{'}_{ads}\left(\frac{1}{L_{fd}} - m_2\right)\right] \quad (2.47)$$

where e_{d0} and e_{q0} can be calculated as

$$e_{d0} = R_E i_{d0} - X_E i_{q0} + E_B \sin\delta_0 \quad (2.48)$$

$$e_{q0} = R_E i_{q0} + X_E i_{d0} + E_B \cos\delta_0 \quad (2.49)$$

i_{d0} and i_{q0} can be obtained from equations (2.27) and (2.28). From the previous expressions the state-space representation of the system is given by

$$\frac{d}{dt}\begin{bmatrix} \Delta\omega_r \\ \Delta\delta \\ \Delta\psi_{fd} \\ \Delta V_c \\ \Delta E_{fd} \end{bmatrix} = \begin{bmatrix} a_{11} & a_{12} & a_{13} & 0 & 0 \\ a_{21} & 0 & 0 & 0 & 0 \\ 0 & a_{32} & a_{33} & 0 & a_{35} \\ 0 & a_{42} & a_{43} & a_{44} & 0 \\ 0 & 0 & 0 & a_{54} & a_{55} \end{bmatrix} \begin{bmatrix} \Delta\omega_r \\ \Delta\delta \\ \Delta\psi_{fd} \\ \Delta V_c \\ \Delta E_{fd} \end{bmatrix} + \begin{bmatrix} b_1 \\ 0 \\ 0 \\ 0 \\ 0 \end{bmatrix} \Delta T_m \quad (2.50)$$

where

$$a_{35} = b_{32} = \frac{\omega_0 R_{fd}}{L_{adu}} \quad (2.51)$$

$$a_{42} = \frac{K_5}{T_R} \quad (2.52)$$

$$a_{43} = \frac{K_6}{T_R} \quad (2.53)$$

$$a_{44} = -\frac{1}{T_R} \quad (2.54)$$

$$a_{54} = -\frac{K_A}{T_A} \quad (2.55)$$

$$a_{55} = -\frac{1}{T_A} \quad (2.56)$$

$$b_1 = b_{11} = \frac{1}{2H} \tag{2.57}$$

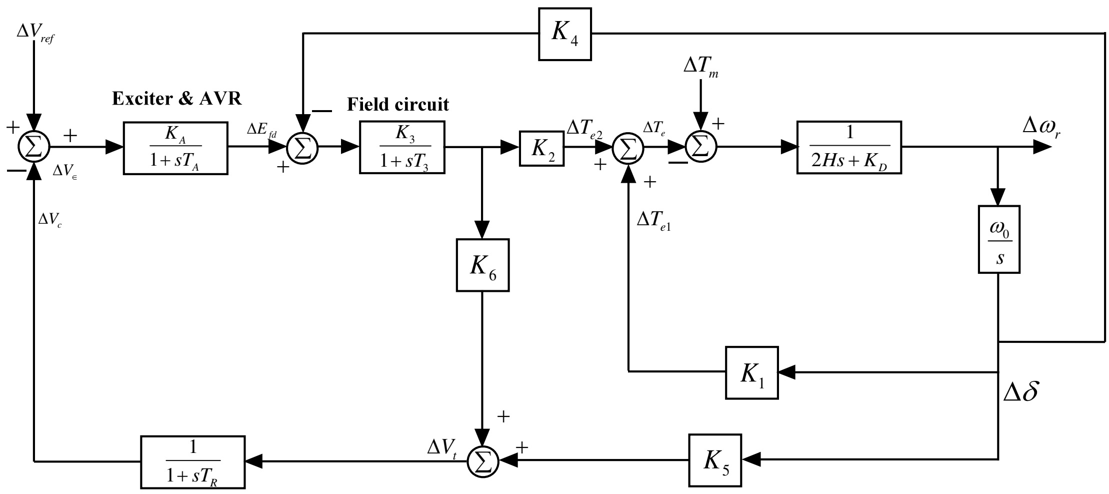

Figure 2.8: Block diagram representation with excitation and AVR

Laplace transformation of equation (2.8) gives

$$\Delta\omega_r = \frac{1}{2Hs + K_D}(\Delta T_m - \Delta T_e) \tag{2.58}$$

The variation of ψ_{fd} is determined by the field circuit dynamic equation, which is given by equation (2.50) as

$$\frac{d}{dt}\Delta\psi_{fd} = a_{32}\Delta\delta + a_{33}\Delta\psi_{fd} + a_{35}\Delta E_{fd} \tag{2.59}$$

Laplace transform of equation (2.59) gives

$$\Delta\psi_{fd} = \frac{K_3}{1 + sT_3}\left[\Delta E_{fd} - K_4\Delta\delta\right] \tag{2.60}$$

where

$$K_3 = -\frac{a_{35}}{a_{33}} \tag{2.61}$$

$$K_4 = -\frac{a_{32}}{a_{35}} \tag{2.62}$$

$$T_3 = -\frac{1}{a_{33}} \tag{2.63}$$

Using equations (2.58), (2.60), (2.45), (2.22) and using Figure 2.7 the block diagram representation of the system including excitation system can be derived and is shown in Figure 2.8. So far the equations derived the constants K_2, K_3 and K_4 are usually positive. As long as K_4 is positive, the effect of field flux variation due to armature reaction is to introduce a positive damping torque component. However there can be situation where K_4 is negative. K_4 is negative where a hydraulic generator without damper windings is operating at light load and is connected by a line of relatively high resistance to reactance ratio to a large system.

Also K_4 can be negative when a machine is connected to a large local load, supplied partly by the generator and partly by the remote large system. Under such conditions, the torques produced by induced currents in the field due to armature reaction has components out of phase with $\Delta\omega$ and produce negative damping.

The coefficient K_6 is always positive, whereas K_5 can either be positive or negative, depending on the operating condition and the external network impedance $R_E + jX_E$. The value of K_5 has a significant bearing on the influence of the AVR on the damping of system oscillations. With K_5 positive, the effect of the AVR is to introduce a negative synchronizing torque and a positive damping torque component. The constant K_5 is positive for low values of external system reactance and low generator outputs.

The reduction in K_s due to AVR action in such cases is usually of no particular concern, because K_1 is so high that the net K_s is significantly greater than zero.

With K_5 negative, the AVR action introduces a positive synchronizing torque component and a negative damping torque component. This effect is more pronounced as the exciter response increases.

For high values of external system reactance and high generator outputs

K_5 is negative. In practice, the situation where K_5 is negative are commonly encountered. For such cases, a high response exciter is beneficial in increasing synchronizing torque. However, in doing so, it introduces negative damping. We thus have conflicting requirement with regard to exciter response. One possible resource is to strike a compromise and set the exciter response so that it results in sufficient synchronizing and damping torque components for the expected range of the system operating conditions. This may not always be possible. It may be necessary to use a high response exciter to provide the required synchronizing toque and system stability performance. With a very high external system reactance, even with low exciter response the net damping torque coefficient may be negative.

With electrical power systems, the change in electrical torque of a synchronous machine, following a small disturbance can be resolved into 2 components.

$\Delta T_e = K_s \Delta\delta + K_D \Delta\omega$

Where $K_s\Delta\delta$, the component of torque change is in phase with the rotor angle perturbation $\Delta\delta$ or called as synchronizing torque component.

$K_D\Delta\omega$, the component of torque change is in phase with the speed deviation $\Delta\omega$ or called as damping torque component.

System stability depends on the existence of both components of torque.

- Lack of sufficient synchronizing torque results in instability through a periodic drift in rotor angle.
- Lack of sufficient damping torque results in oscillatory instability.

For a generator connected radially to a large power system, in the absence of automatic voltage regulator (i.e. with constant field voltage), the instability is due to the lack of sufficient synchronizing torque (i.e. -ve K_s). This results in instability through a non-oscillatory mode. For +ve values of K_s, the synchronizing torque component opposes changes in the rotor angle from the equilibrium point (i.e. an increase in the rotor angle will lead to a net decelerating torque, until the rotor angle is restored to its equilibrium point ($\Delta\delta = 0$)). Similarly for +ve values of K_D the damping torque component opposes changes in the rotor speed from the steady-state operating point.

For a generator connected radially to a large power system, in the presence of automatic voltage regulator, the instability is due to the lack of sufficient damping torque. This results in instability through an oscillatory mode. A number of factors can influence the damping coefficient of a synchronous generator; including the generator's design, the strength of the machine's interconnection to the grid and the setting of the excitation system. With -ve damping torque causes the electromechanical oscillations to grow and eventually causing loss of synchronism. This form of instability is normally referred to as dynamic, small-signal or oscillatory instability to differentiate it from the steady-state stability and transient stability.

For a generator connected radially to a large power system, in the presence of automatic voltage regulator, the instability is due to the lack of sufficient damping torque (i.e. -ve K_D). This results in instability through an oscillatory mode. A number of factors can influence the damping coefficient of a synchronous generator including the generator's design, the strength of the machine's interconnection to the grid and the setting of the excitation system. With -ve damping torque (i.e. -ve K_D) causes the electromechanical oscillations to grow and eventually causing loss of synchronism. This form of instability is normally referred to as dynamic, small-signal or oscillatory instability to differentiate it from the steady-state stability and transient stability.

2.6 Prime Mover and Governing System Models

The prime mover governing system provides a means of controlling real power and frequency. A basic characteristic of a governor is shown in Figure 2.9.

Form the Figure 2.9, there is a definite relationship between the turbine speed and the load being carried the turbine for a given setting. The increase

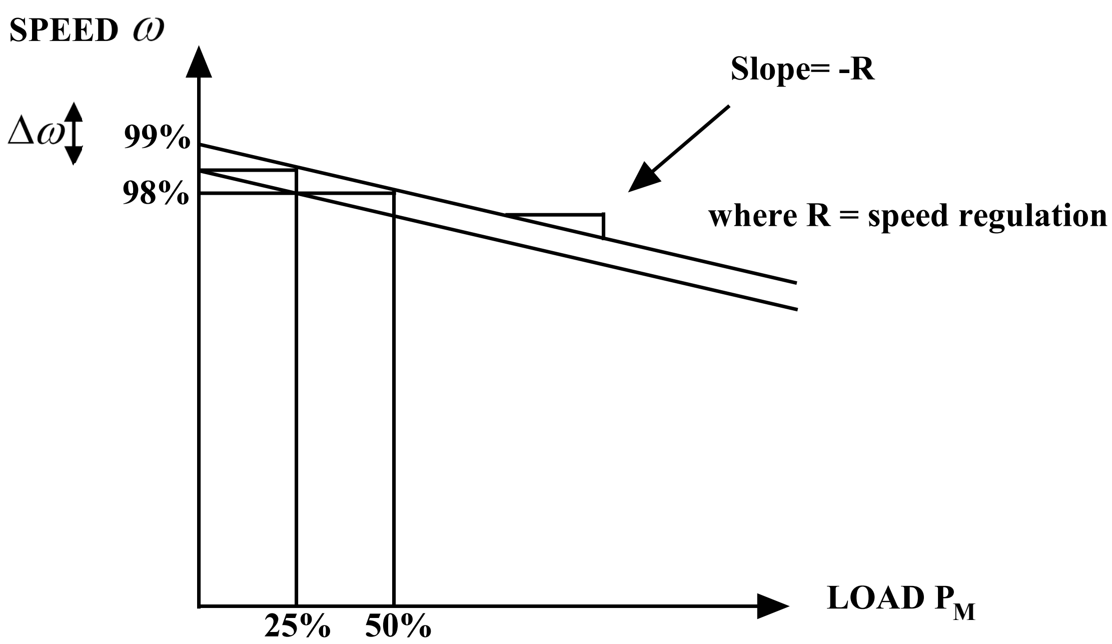

Figure 2.9: Governor Characteristic

in load will lead to a decrease in speed. The example given in Figure 2.9 shows that if the initial operating is at and the load is dropped to 25 percent, the speed will increase. In order to maintain the speed at , the governor setting by changing the spring tension in the fly ball type of governor will be resorted to and the characteristic of the governor will be indicated by the dotted line as shown in Figure 2.9.

Figure 2.9 illustrates the ideal characteristic of the governor whereas the actual characteristic departs from the ideal one due to valve openings at different loadings. In contrast to the excitation system, the governing system is a relatively slow response system because of the slow reaction of mechanic operation of turbine machine.

In Figure 2.10, the schematic diagram of a speed governing system that controls the real power flow in the power system is shown.

As shown, the speed governor is made up of the following parts:

- Speed governor: This is a fly ball type of speed governor. The mechanism provides upward and downward vertical movements proportional to the

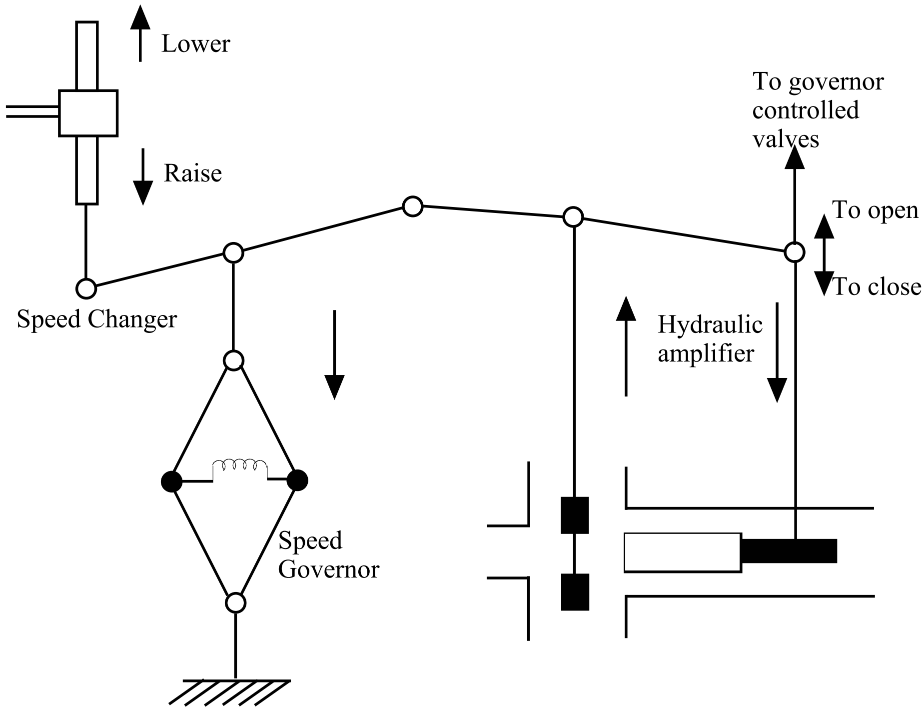

Figure 2.10: Speed governing system

change in speed.

- Linkage mechanism: Provide a movement to the control valve in the proportion to change in speed.
- Hydraulic amplifier: Low power level pilot valve movement is converted into high power level piston valve movement which is necessary to open or close the steam valve against high pressure steam.
- Speed Changer: Provides a steady-state power output setting for the turbine.

When selecting a prime mover to model in a simulation, special considerations are required as different types of turbine required different operating conditions and hence the effects on the power system stability will be different. Using an example of hydraulic turbines, a large transient (temporary) droop with a long resettling time is needed for stable control performance because of the "water hammer" effect; a change in gate position generates an initial turbine power change which is opposite that which is desired. The transient droop provides a transient gain reduction compensation that limits the gate movement until the water flow and power outputs have time to catch up. Figure 2.11 describes the process using block diagram.

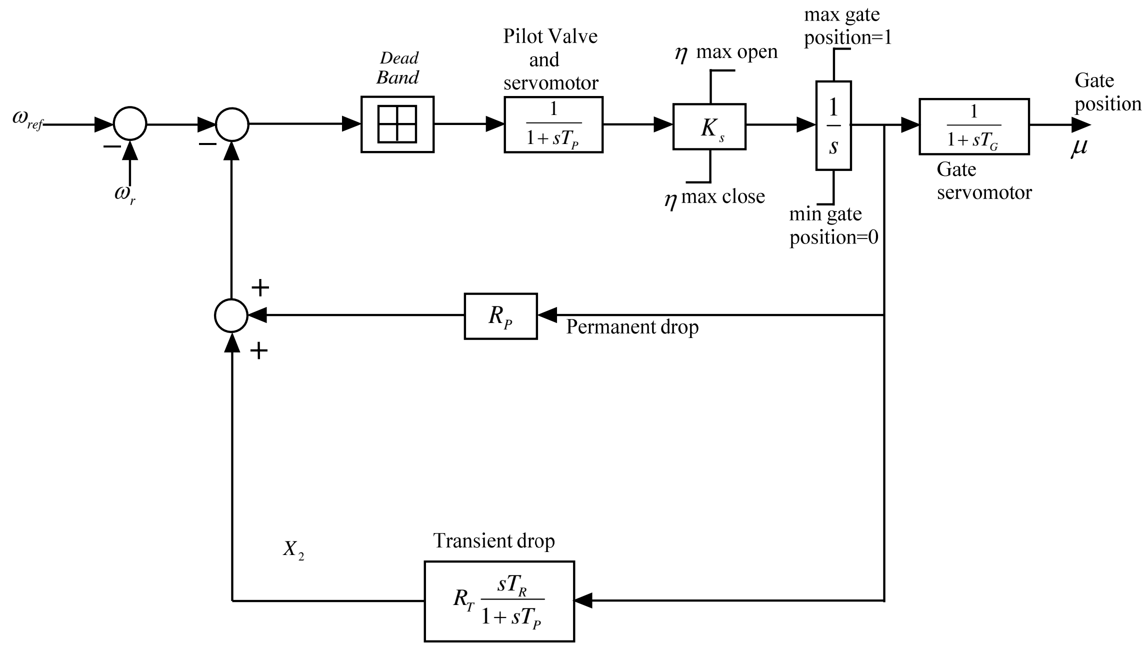

Figure 2.11: Block diagram of a governing system for a hydraulic turbine

2.7 Power System Stabilizer (PSS) Model

The basic function of a power system stabilizer is to add damping to the generator rotor oscillations by controlling its excitation using auxiliary stabilizing signal(s). To provide damping, the stabilizer must produce a component of electrical torque in phase with the rotor speed deviations.

It is well established that fast acting exciters with high gain AVR can contribute to oscillatory instability in power systems. This type of instability is characterized by low frequency (0.2 to 2.0 Hz) oscillations which can persist (or even grow in magnitude) for no apparent reason. This type of instability can endanger system security and limit power transfer. The major factors that contribute to the instability are

- Loading of the generator or tie line
- Power transfer capability of transmission lines
- Power factor of the generator (leading power factor operation is more problematic than lagging power factor operation)
- AVR gain

A cost efficient and satisfactory solution to the problem of oscillatory instability is to provide damping for generator rotor oscillations. This is conveniently done by providing Power System Stabilizers (PSS) which are supplementary controllers in the excitation systems. The objective of designing PSS is to provide additional damping torque without affecting the synchronizing torque at critical oscillation frequencies. It can be generally said that need for PSS will be felt in situations when power has to be transmitted over long distances with weak AC ties. Even when PSS may not be required under normal operating conditions, they allow satisfactory operation under unusual or abnormal conditions which may be encountered at times. Thus, PSS has become a standard option with modern static exciters and it is essential for power engineers to use these effectively. Retrofitting of existing excitation systems with PSS may also be required to improve system stability.

The theoretical basis for a PSS may be illustrated with the aid of the block diagram shown in Figure 2.12. This is an extension of the block diagram shown in Figure 2.8 and includes the effects of a PSS. Since the purpose of a PSS is to introduce a damping torque component, a logical signal to use for controlling generator excitation is the speed deviation $\Delta\omega_r$.

If the exciter transfer function and the generator transfer function between ΔE_{fd} and ΔT_e were pure gains, a direct feedback of $\Delta\omega_r$ would result in a damping torque component. However, in practice both the generator and the exciter exhibit frequency dependent gain and phase characteristics. Therefore, the PSS transfer function $G_{pss}(s)$ should have appropriate phase compensation circuits to compensate for the phase lag between the exciter

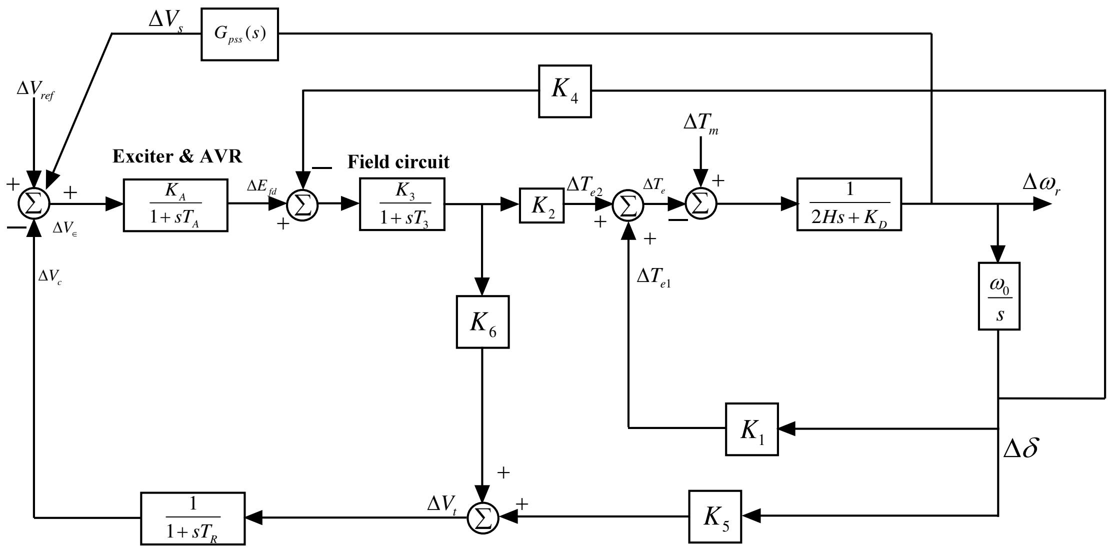

Figure 2.12: Block diagram of thyristor excitation system with AVR and PSS

input and the electrical torque. In the ideal case, with the phase characteristic of $G_{pss}(s)$ being an exact inverse of the exciter and generator phase characteristics to be compensated, the PSS would result in a pure damping torque at all oscillating frequencies.

Figure 2.12 shows the block diagram of the excitation system, including the AVR and PSS. The PSS representation in Figure 2.13 consists of three blocks: a phase compensation block, a signal washout block, and a gain block.

The phase compensation block provides the appropriate phase lead characteristic to compensate for the phase lag between the exciter input and the generator electrical (air-gap) torque. The figure shows a single first-order block. In practice, two or more first-order blocks may be used to achieve the desired phase compensation. In some cases, second-order blocks with complex roots have been used.

Normally, the frequency range of interest is 0.1 to 2.0 Hz and the phase-lead network should provide compensation over this entire frequency range. The phase characteristic to be compensated changes with system conditions; therefore a compromise is made and a characteristic is acceptable for different system conditions is selected. Generally some under compensation is

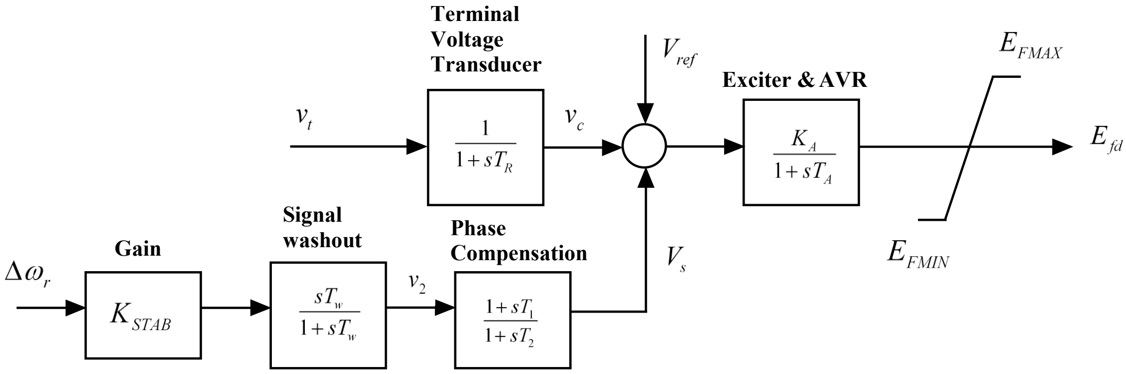

Figure 2.13: Block diagram of thyristor excitation system with AVR and PSS

desirable so that the PSS, in addition to significantly increase the damping torque, results in a slight increase of the synchronizing torque.

The signal washout block serves as a high-pass filter, with the time constant T_w high enough to allow signals associated with oscillations in ω_r to pass unchanged. Without it, steady changes in speed would modify the terminal voltage. It allows the PSS to respond only to changes in speed. From the view point of the washout function, the value of T_w is not critical and may be in the range of 1 to 20 seconds. The main consideration is that it be long enough to pass stabilizing signals at the frequencies of interest unchanged, but not so long that it leads to undesirable generator voltage excursions during system-islanding conditions.

The stabilizer gain determines the amount of damping introduced by the PSS. Ideally, the gain should be set at a value corresponding to maximum damping; however it is often limited by other considerations.

From Figure 2.13, using perturbed values, we have

$$\Delta v_2 = \frac{pT_w}{1 + pT_w}(K_{STAB}\Delta\omega_r) \tag{2.64}$$

Hence

$$p\Delta v_2 = K_{STAB}p\Delta\omega_r - \frac{1}{T_w}\Delta v_2 \tag{2.65}$$

Substituting for $p\Delta\omega_r$ by equation (2.31), we obtain the expression for $p\Delta v_2$ in terms of the state variables.

$$p\Delta v_2 = K_{STAB}\left[a_{11}\Delta\omega_r + a_{12}\Delta\delta + a_{13}\Delta\psi_{fd} + \frac{1}{2H}\Delta T_m\right] - \frac{1}{T_w}\Delta v_2$$

$$= a_{51}\Delta\omega_r + a_{52}\Delta\delta + a_{53}\Delta\psi_{fd} + a_{55}\Delta v_2 + \frac{K_{STAB}}{2H}\Delta T_m \quad (2.66)$$

where

$$a_{51} = K_{STAB}a_{11} \quad (2.67)$$

$$a_{52} = K_{STAB}a_{12} \quad (2.68)$$

$$a_{53} = K_{STAB}a_{13} \quad (2.69)$$

$$a_{55} = -\frac{1}{T_w} \quad (2.70)$$

Since $p\Delta v_2$ is not a function of Δv_c and Δv_3, $a_{54} = a_{56} = 0$

$$\Delta v_s = \Delta v_2\left(\frac{1 + pT_1}{1 + pT_2}\right) \quad (2.71)$$

Hence

$$p\Delta v_s = \frac{T_1}{T_2}p\Delta v_2 + \frac{1}{T_2}\Delta v_2 - \frac{1}{T_2}\Delta v_s \quad (2.72)$$

Substitution for $p\Delta v_2$, given by equation (2.66), yields

$$p\Delta v_s = a_{61}\Delta\omega_r + a_{62}\Delta\delta + a_{63}\Delta\psi_{fd} + a_{64}\Delta v_c + a_{65}\Delta v_2 + a_{66}\Delta v_s + \frac{T_1}{T_2}\frac{K_{STAB}}{2H}\Delta T_m \quad (2.73)$$

where

$$a_{61} = \frac{T_1}{T_2}a_{51} \quad (2.74)$$

$$a_{62} = \frac{T_1}{T_2}a_{52} \quad (2.75)$$

$$a_{63} = \frac{T_1}{T_3} a_{53} \tag{2.76}$$

$$a_{65} = \frac{T_1}{T_2} a_{55} + \frac{1}{T_2} \tag{2.77}$$

$$a_{66} = -\frac{1}{T_2} \tag{2.78}$$

From Figure 2.12 we have

$$\Delta E_{fd} = K_A(\Delta v_s - \Delta v_c) \tag{2.79}$$

The field circuit equation, with PSS included becomes

$$p\Delta\psi_{fd} = a_{32}\Delta\delta + a_{33}\Delta\psi_{fd} + a_{34}\Delta v_c + a_{36}\Delta v_s \tag{2.80}$$

where

$$a_{36} = \frac{\omega_0 R_{fd}}{L_{adu}} K_A \tag{2.81}$$

The complete state-space model, including the PSS, has the following form (with$\Delta T_m = 0$)

$$\begin{bmatrix} \Delta\omega_r \\ \Delta\delta \\ \Delta\psi_{fd} \\ \Delta v_c \\ \Delta v_2 \\ \Delta v_s \end{bmatrix} = \begin{bmatrix} a_{11} & a_{12} & a_{13} & 0 & 0 & 0 \\ a_{21} & 0 & 0 & 0 & 0 & 0 \\ 0 & a_{32} & a_{33} & a_{34} & 0 & a_{36} \\ 0 & a_{42} & a_{43} & a_{44} & 0 & 0 \\ a_{51} & a_{52} & a_{53} & 0 & a_{55} & 0 \\ a_{61} & a_{62} & a_{63} & 0 & a_{65} & a_{66} \end{bmatrix} \begin{bmatrix} \Delta\omega_r \\ \Delta\delta \\ \Delta\psi_{fd} \\ \Delta v_c \\ \Delta v_2 \\ \Delta v_s \end{bmatrix} \tag{2.82}$$

The PSS parameters should be such that the control system results into the following.

- Maximize the damping of the local plant mode as well as inter-area mode oscillations without compromising stability of other modes.
- Enhance system transient stability

- Not adversely affect system performance during major system upsets which cause large frequency excursions
- Minimize the consequences of excitation system malfunction due to component failure.

Chapter 3

CONVENTIONAL POWER SYSTEM STABILIZERS

3.1 Introduction

In this chapter, a conventional power system stabilizer is designed on the basis of the block diagram representation of the system introduced in chapter 2. Here the design procedure is performed in the frequency domain. Conventional power system stabilizers (CPSSs) are basically designed on the basis of a linear model for the power system. The power system is first linearised around a specific operating point of the system. Then, assuming that disturbances are small such that the linear model remains valid, the CPSS is designed. Therefore, a CPSS is most useful for preserving dynamic stability of the power system.

3.2 Conventional Power System Stabilizer Design

The basic function of a PSS is to add damping to the generator rotor oscillations by controlling its excitation using auxiliary stabilizing signal. To provide damping, the stabilizer must produce a component of electrical torque in phase with the rotor speed deviation.

For the simplicity a conventional PSS is modelled by two stage (identical), lead/lag network which is represented by a gain K_{STAB} and two time constants T_1 and T_2. This network is connected with a washout circuit of a time constant T_w as shown in Figure 3.1.

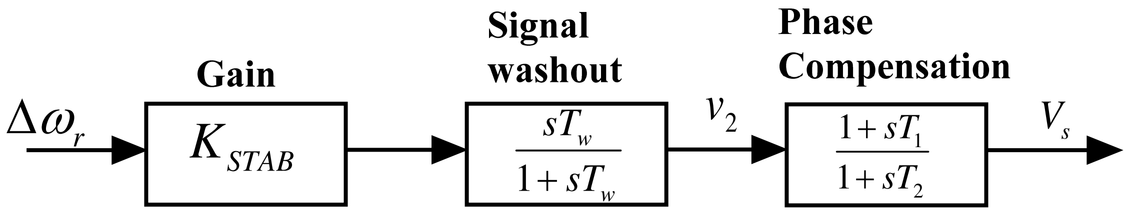

Figure 3.1: Block diagram of PSS

In Figure 3.1 the phase compensation block provides the appropriate phase lead characteristics to compensate for the phase lag between exciter input and generator electrical torque. The phase compensation may be a single first order block as shown in Figure 3.1 or having two or more first order blocks or second order blocks with complex roots.

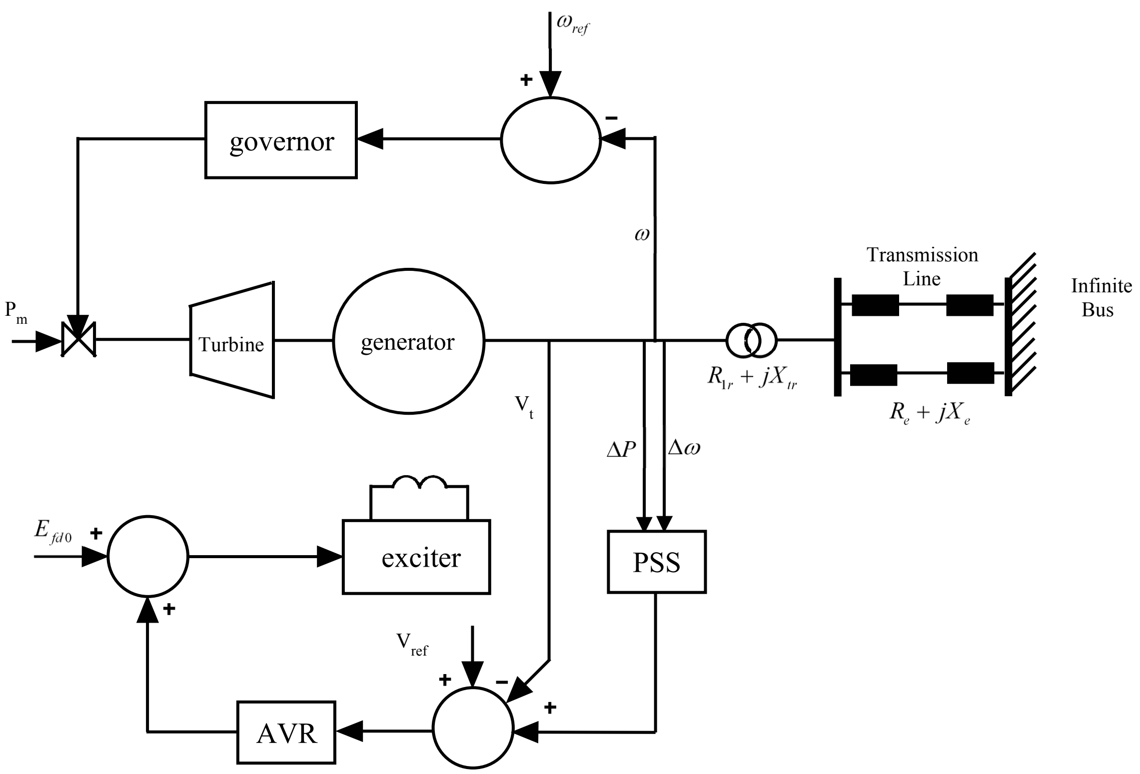

Figure 3.2: Power System Configuration

The signal washout block serves as high pass filter, with time constant T_w high enough to allow signals associated with oscillations in ω_r to pass unchanged, which removes d.c. signals. Without it, steady changes in speed would modify the terminal voltage. It allows PSS to respond only to changes in speed.

The stabilizer gain K_{STAB} determines the amount of damping introduced by PSS. Ideally, the gain should be set at a value corresponding to maximum damping; however, it is limited by other consideration.

The block diagram of a single machine infinite bus (SMIB) system, which illustrates the position of a PSS, is shown in Figure 3.2.

The system consists of a generating unit connected to an infinite bus through a transformer and a pair of transmission lines. An excitation system and automatic voltage regulator (AVR) are used to control the terminal voltage of the generator. An associated governor monitors the shaft frequency and controls mechanical power.

Adding a PSS to the block diagram shown in Figure 2.8, the block diagram of the power system with PSS is obtained as shown in Figure 3.3. Since the

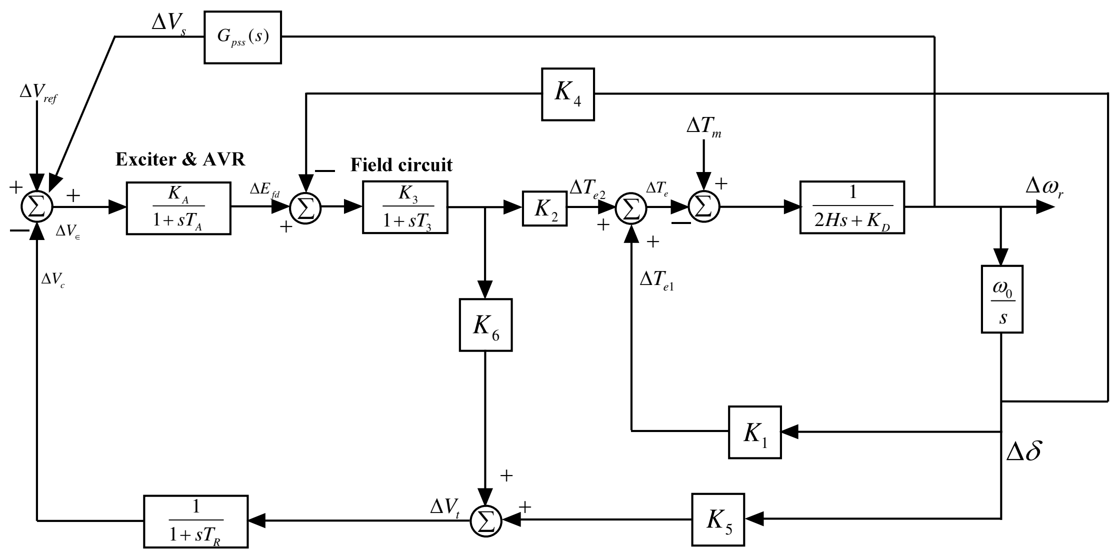

Figure 3.3: Block diagram of a linear model of a synchronous machine with a PSS

purpose of a PSS is to introduce a damping torque component, a logical signal to use as the input of PSS is $\Delta\omega_r$. If the exciter transfer function and the generator transfer function between ΔE_{fd} and ΔT_e were pure gains, a direct feedback of $\Delta\omega_r$ would result in a damping torque component. However, both transfer functions between ΔE_{fd} and ΔT_e exhibit frequency dependent gain and phase characteristics. Therefore, the CPSS transfer function should have an appropriate phase compensation circuit to compensate for the phase lag between the exciter input and the electrical torque. In the ideal case, with the phase characteristics of $G_{pss}(s)$ being an exact inverse of the exciter and generator phase characteristics, the CPSS would result in a pure damping torque at all oscillating frequencies.

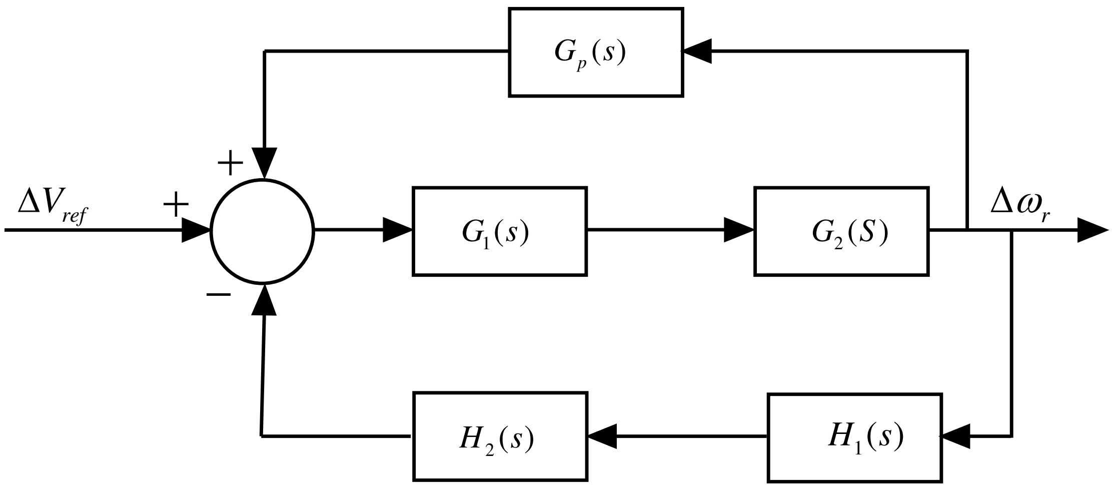

Figure 3.4: Simplified block diagram to design a CPSS

The block diagram of Figure 3.3 can be reduced to the block diagram shown in Figure 3.4, where

$$G_1(s) = \frac{K_A K_3}{T_A T_3 s^2 + (T_A T_3)s + 1} \tag{3.1}$$

$$G_2(s) = \frac{K_2 K_3 s^2 + K_2 s}{2HT_3 s^2 + (2H + K_d T_3)s^2 + (K_1 T_3 \omega_0 + K_d)s + \omega_0(K_1 - K_2 K_3 K_4)} \tag{3.2}$$

$$H_1(s) = \frac{-2K_6Hs^2 - K_6K_ds + \omega_0(K_2K_5 - K_1K_6)}{K_2s} \tag{3.3}$$

$$H_2(s) = \frac{1}{1 + sT_R} \tag{3.4}$$

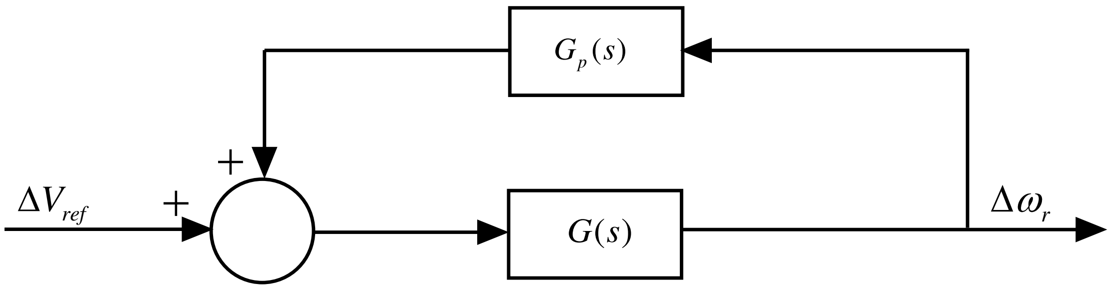

Figure 3.5: Compact block diagram to design a CPSS

The block diagram in Figure 3.4 can be simplified to the block diagram shown in Figure 3.5.

$$G(s) = \frac{G_1(s)G_2(s)}{1 + G_1(s)G_2(s)H_1(s)H_2(s)} \tag{3.5}$$

which is expanded to

$$G(s) = \frac{-K_AK_3(K_3s + 1)}{a_6s^6 + a_5s^5 + a_4s^4 + a_3s^3 + a_2s^2 + a_1s + a_0} \tag{3.6}$$

where

$$a_6 = 2T_AT_RT_3^2H \tag{3.7}$$

$$a_5 = T_3[2K_AT_3H + K_AT_R(2H + K_dT_3) + 2T_RH(T_A + T_3)] \tag{3.8}$$

$$a_4 = (2H+K_dT_3)[K_AT_3+T_R(T_A+T_3)]+2T_3H(T_A+T_3+T_R)+T_AT_3T_R(K_1T_3\omega_0+K_d) \tag{3.9}$$

$$a_3 = (K_1 T_3 \omega_0 + K_d)[T_A T_3 + T_R(T_A + T_3)] + (2H + K_d T_3)(T_A + T_3 + T_R) + 2H(T_3 + K_A K_3^2 K_6) + T_A T_3 T_R \omega_0 (K_1 - K_2 K_3 K_4) \tag{3.10}$$

$$a_2 = (T_A + T_3 + T_R)(K_1 T_3 \omega_0 + K_d) + \omega_0 (K_1 - K_2 K_3 K_4)[T_A T_3 + T_R(T_A + T_3)] + K_6(2H + K_A K_d K_3^2) + 2H + K_d T_3 \tag{3.11}$$

$$a_1 = \omega_0 (K_1 - K_2 K_3 K_4)(T_A + T_3 + T_R) + K_A K_3^2 \omega_0 (K_1 K_6 - K_5) + K_d(K_6 + 1) + K_1 T_3 \omega_0 \tag{3.12}$$

$$a_0 = \omega_0 [K_1(K_6 + 1) - K_2(K_5 + K_3 K_4)] \tag{3.13}$$

The CPSS is designed for the normal operating point, i.e., $P_0 = 0.8$ pu, with a lagging power factor of 0.8 and $E_B = 1.0$ pu, where P_0 is the generated active power and E_B is the infinite bus voltage. Here the frequency response method is used to design the CPSS. Bode plot of the plant without PSS (G(s)) for this operating condition is shown in Figure 3.6.

As shown in the Figure 3.6, a response occurs at ω_r= 10 rad/sec. That's why if there is a step change in V_{ref}, the rotor speed will oscillate around the synchronous speed. So a PSS is required to damp the oscillations.

The CPSS is constructed of two lead stages cascaded with a wash-out term, with the following transfer function:

$$G_p(s) = K_{STAB} \frac{sT_w}{1 + sT_w} \left(\frac{1 + sT_1}{1 + sT_2} \right) \tag{3.14}$$

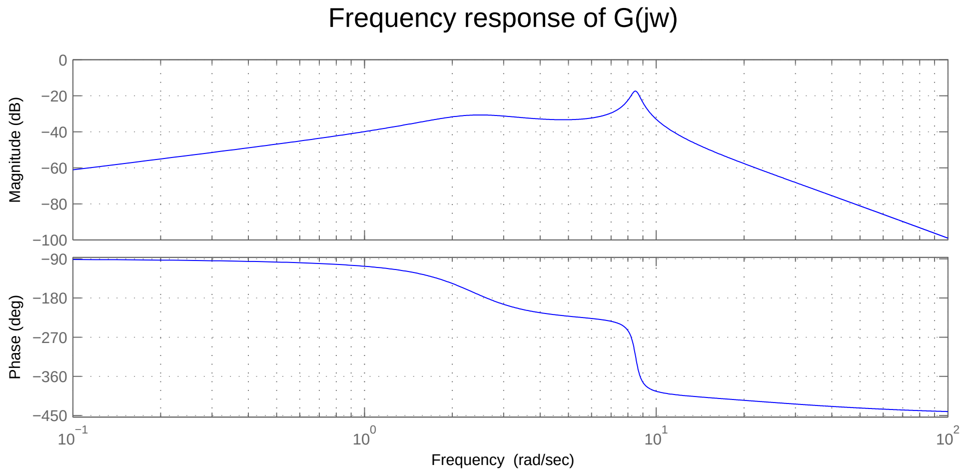

Figure 3.6: Frequency response of the plant without PSS

The first term in equation (3.14) is a high pass filter that is used to "wash out" the compensation effect for very low-frequency signals. It attenuates signals with angular frequency less than $\frac{1}{T_w}$ rad/sec. The use of this term will assure no permanent offset in the terminal voltage due to prolonged error in the power system frequency, such as might occur in an overload or islanding condition. The second term is a lead compensation pair that is used to compensate for the phase lag through the system.

The CPSS is a compensator in the feedback path of the system. For the case of cascade (series) compensation the effect of the controller on the closed-loop transfer function is directly determined. However, the effect of the feedback compensator on the closed-loop transfer function of the system is not easily determined. Therefore, techniques for developing feedback compensators are different and usually more involved than those for developing cascade compensators.

The overall transfer function of the system with the PSS is:

$$G_1(j\omega) = \frac{G(j\omega)}{1 - G(j\omega)G_p(j\omega)} \tag{3.15}$$

The overall transfer function can be approximated by

$$G_1(j\omega) \approx G(j\omega) for (|G(j\omega)G_p(j\omega)| \ll 1) \tag{3.16}$$

and

$$G_1(j\omega) \approx \frac{1}{G_p(j\omega)} for(|G(j\omega)G_p(j\omega)| \gg 1) \tag{3.17}$$

The condition when $|G(j\omega)G_p(j\omega)| \approx 1$ is still undefined, in which case neither equation (3.16) nor equation (3.17) is applicable. In the design procedure, this condition is neglected. The aforementioned approximations allow investigation of the qualitative results to be obtained. After the design of $G_p(s)$ is completed, the closed-loop frequency response of the whole system will be obtained and the designer will make sure that the stabilizer performance is satisfactory in the frequency design of interest.

Thus, $G_p(s)$ should be designed such that:

- $|G(j\omega)G_p(j\omega)| \gg 1$ in the vicinity of the resonance region of the system. This means that the overall transfer function of the system will be approximately equal to $-\frac{1}{G_p(j\omega)}$ in the resonance region of the system. Therefore, gain and phase responses of $-\frac{1}{G_p(j\omega)}$ should be desirable in that region.
- $\frac{1}{|G_p(j\omega)|}$ is considerably less than $|G(j\omega)|$ in that region.
- Phase of $G(j\omega)G_p(j\omega)$ is approximately equal to -180 degrees in that region. This means that the output of $G_p(s)$ will have an opposite phase with respect to the input to $G(s)$ causing a negative feedback (notice positive signs of the comparator inputs in Figure 3.4). For this to happen, $G_p(s)$ must be a lead compensator.

Taking the above situations into consideration, the CPSS is designed. The designed values are K_{STAB}= 20, T_w=1.4 sec, T_1=0.154 sec, T_2=0.033 sec. Figure 3.7 shows the frequency response of the CPSS.

Figure 3.8 shows the log magnitude of ${}^{1}\!/_{G_p(j\omega)}$ placed over log magnitude of $G(j\omega)$.

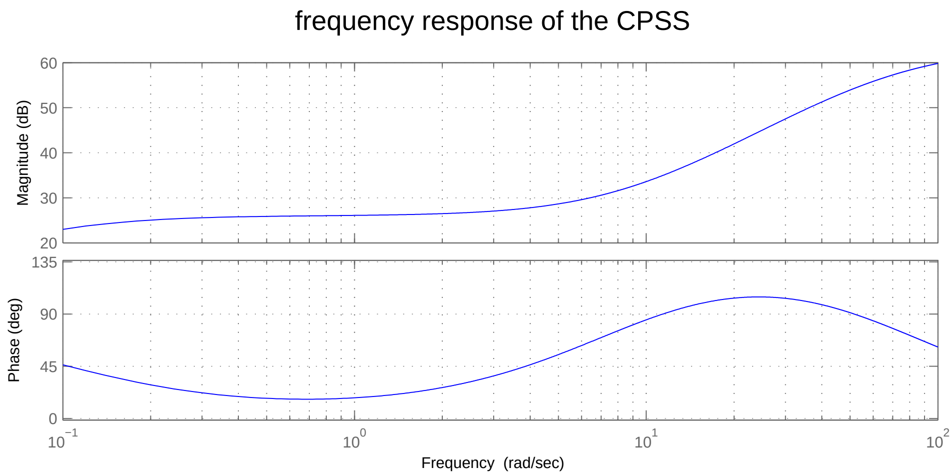

Figure 3.7: Frequency response of the CPSS ($G_p(j\omega)$)

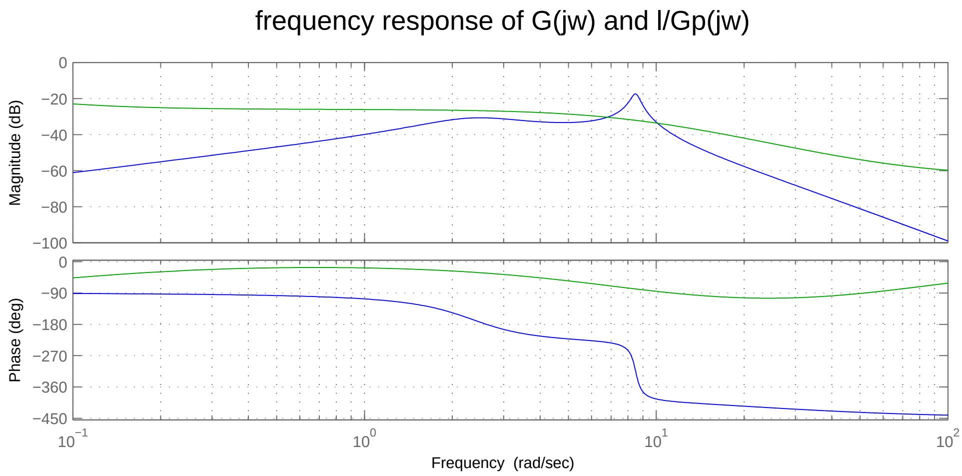

Figure 3.8: Frequency response of log magnitude of $G(j\omega)$ and $^1\!/_{G_p(j\omega)}$

By applying the designed $G_p(s)$ to the system, the closed loop frequency response will be obtained as Figure 3.9.

From Figure 3.9 it shows that the sharp resonance which was observed in Figure 3.6 is made smooth with a smaller magnitude and it occurs at a smaller frequency.

3.3 Conclusion

The Conventional power system stabilizer (CPSS) damps the low frequency oscillations in the shaft speed of a synchronous machine. Since the design is on the basis of a block diagram of the system derived for a specific op-

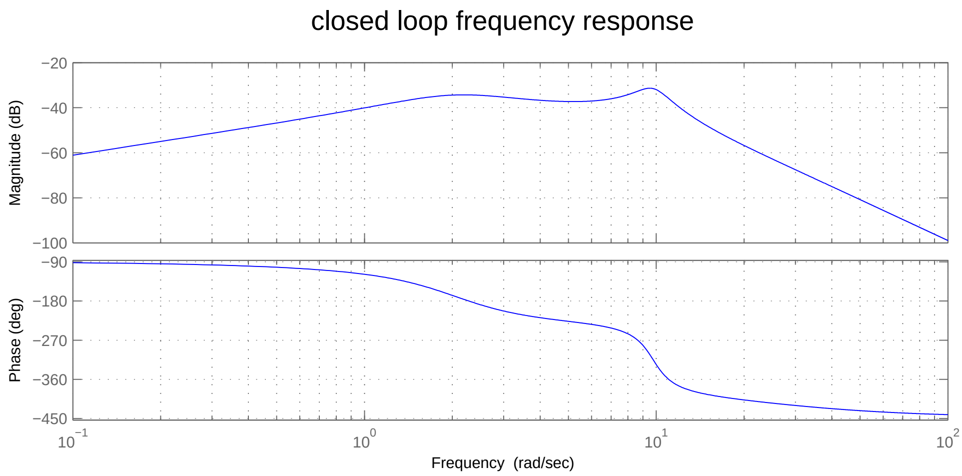

Figure 3.9: Closed loop frequency response of the system with CPSS

erating point, the CPSS has the best response for this operating point. If the operating point of the system changes, the performance of the CPSS will degrade.

Chapter 4

DESIGN OF FUZZY LOGIC BASED PSS

4.1 Introduction

In 1965, Lofty A. Zadeh of the University of California at Berkeley published "Fuzzy Sets" which laid out the mathematics of fuzzy set theory and, by extension, fuzzy logic. Zadeh had observed that conventional computer logic couldn't manipulate data that represented subjective or vague ideas, so he created fuzzy logic to allow computers to determine the distinctions among data with shades of gray, similar to the process of human reasoning. Fuzzy logic, as its name suggests, is the logic underlying modes of reasoning which are approximate rather than exact.

FLCs are very useful when an exact mathematical model of the plant is not available; however, experienced human operators are available for providing qualitative rules to control the system. Fuzzy logic, which is the logic on which fuzzy logic control is based, is much closer in spirit to human thinking and natural language than the traditional logic systems. Basically, it provides an effective mean of capturing the approximate, inexact nature of our knowledge about the real world. Viewed in this perspective, the essential part of the fuzzy logic controller (FLC) is a set of linguistic control rules related by dual concepts of fuzzy implication and the compositional rule of inference.

In essence, the FLC provides an algorithm which can convert the linguistic control strategy based on expert knowledge into an automatic control strategy. The methodology of the FLC appears very useful when the processes are too complex for analysis by conventional quantitative techniques.

Fuzzy logic is a derivative from classical Boolean logic and implements soft linguistic variables on a continuous range of truth values to be defined between conventional binary i.e. [0, 1]. It can often be considered a subset of conventional set theory. The fuzzy logic is capable to handle approximate information in a systematic way and therefore it is suited for controlling nonlinear systems and for modeling complex systems where an inexact model exists or systems where ambiguity or vagueness is common.

The importance of fuzzy logic derives from the fact that most modes of human reasoning and especially common sense reasoning are approximate in nature. In doing so, the fuzzy logic approach allows the designer to handle efficiently very complex closed-loop control problems. There are many artificial intelligence techniques that have been employed in modern power systems, but fuzzy logic has emerged as the powerful tool for solving challenging problems. As compared to the conventional PSS, the Fuzzy Logic Controller (FLC) has some advantages such as:

- A simpler and faster methodology.
- It does not need any exact system mathematical model.
- It can handle nonlinearity of arbitrary complexity.
- It is based on the linguistic rules with an IF-THEN general structure, which is the basis of human logic.
- It is more robust than conventional nonlinear controllers.

4.2 Fuzzy sets

Fuzzy set, as the name implies, is a set without a crisp boundary. The transition from "belong to a set" to "not belong to a set" is gradual, and this smooth transition is characterized by membership functions. The fuzzy set theory is based on fuzzy logic, where a particular object has a degree of membership in a given set that may be anywhere in the range of 0 to 1. On the other hand, classical set theory is based on Boolean logic, where a particular object or variable is either a member of a given set (logic 1), or it is not (logic 0).

4.3 Membership functions

A membership function is a curve that defines how the values of a fuzzy variable in a certain region are mapped to a membership value μ (or degree of membership) between 0 and 1. The MF maps each element of X to a membership degree between 0 and 1 (included). Obviously, the definition of a fuzzy set is a simple extension of the definition of a classical (crisp) set in which the characteristic function is permitted to have any value between 0 and 1. If the value of the membership function is restricted to either 0 or 1, then A is reduced to a classical set. For clarity, we shall also refer to classical sets as ordinary sets, crisp sets, non-fuzzy sets, or just sets. Usually, X is referred to as the universe of discourse, or simply the universe, and it may consist of discrete (ordered or non-ordered) objects or it can be a continuous space. In practice, when the universe of discourse X is a continuous space, we usually partition it into several fuzzy sets whose MFs cover X in a more or less uniform manner. These fuzzy sets, which usually carry names that conform to adjectives appearing in our daily linguistic usage, such as "large," "medium," or "small," are called linguistic values or linguistic labels. Thus, the universe of discourse X is often called the linguistic variable. The fuzzy membership not only provides for a meaningful and powerful representation of measurement of uncertainties, but also provides the meaningful representation of vague concepts expressed in natural language. If X is a collection of objects denoted generically by x, then a fuzzy set in X is defined as a set of ordered pairs.

$$A = \{(x, \mu_A(x))/x \varepsilon X\} \tag{4.1}$$

where $\mu_A(x)$ is called the membership function for the set A. There exist different shapes of membership functions. The shapes could be triangular, trapezoidal, curved or their variations.

The various types of membership functions are given below.

4.3.1 Triangular Membership Function

A triangular membership function is specified by three parameters $\{a, b, c\}$ as follows:

$$f(x; a, b, c) = \begin{cases} 0, & x \leq a \\ \frac{x-a}{b-a}, & a \leq x \leq b \\ \frac{c-x}{c-b}, & b \leq x \leq c \\ 0, & c \leq x \end{cases} \tag{4.2}$$

The parameters a and c locate the feet of the triangle and the parameter b

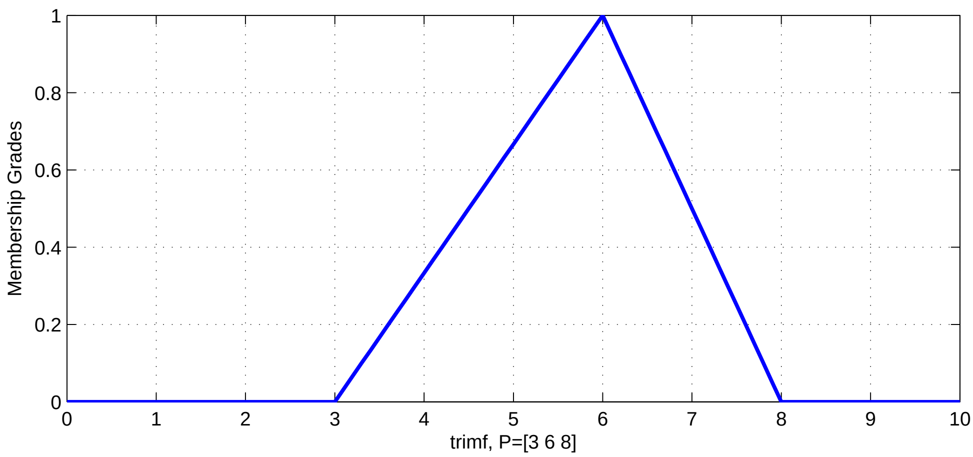

Figure 4.1: Triangular Membership Function

locate the peak.

For example the triangular membership function trimf (x; 3, 6, 8) can be illustrated as shown in Figure 4.1.

4.3.2 Gaussian Membership Function

A Gaussian membership function is specified by two parameters$\{c, \sigma\}$:

$$gaussmf(x; c, \sigma) = e^{-\frac{1}{2}\left(\frac{x-c}{\sigma}\right)^2} \tag{4.3}$$

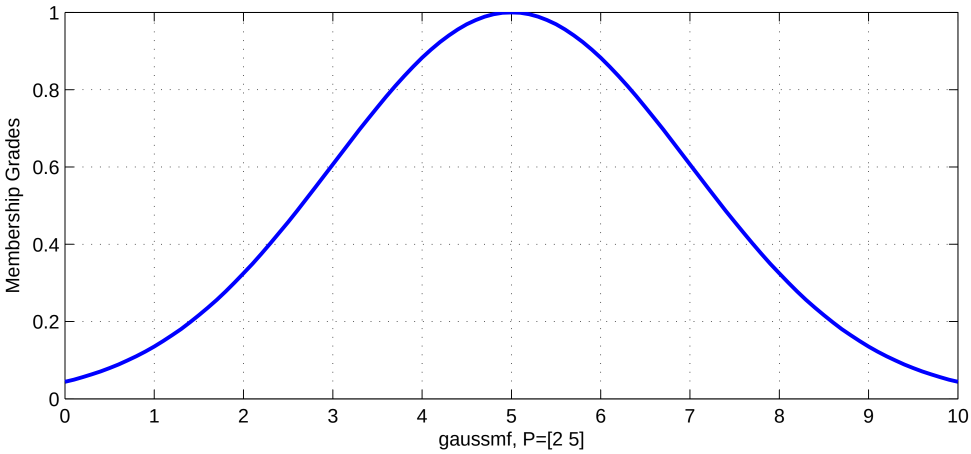

Figure 4.2: Gaussian Membership Function

A Gaussian membership function is determined completely by c and σ; c represents the MFs centre and σ determines the MFs width.

Figure 4.2 plots a Gaussian membership function defined by gaussmf (x, 2, 5)

4.3.3 Trapezoidal Membership Function

A Trapezoidal membership function is specified by four parameters

$$f(x; a, b, c, d) = \begin{cases} 0, & x \leq a \\ \frac{x-a}{b-a}, & a \leq x \leq b \\ 1, & b \leq x \leq c \\ \frac{d-x}{d-c}, & c \leq x \leq d \\ 0, & d \leq x \end{cases} \tag{4.4}$$

The parameters a and d locates the feet of the trapezoid and the parameters b and c locates the shoulders.

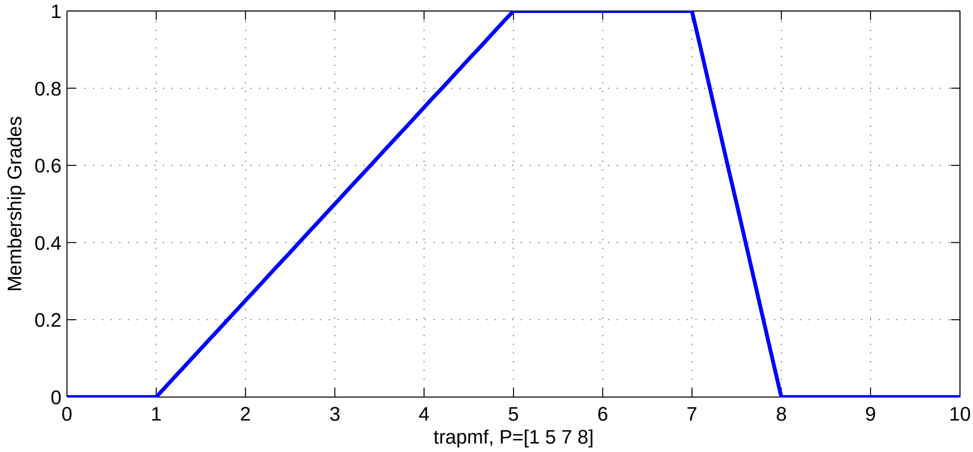

Figure 4.3: Trapezoidal Membership Function

For example the Trapezoidal membership function defined by trapmf (x, 2, 5) can be illustrated as shown in Figure 4.3.

In real time implementation, both the triangular membership function and trapezoidal membership function have been used extensively due to their simple formulas and computational efficiency. These two membership functions can have symmetrical or unsymmetrical shape.

4.3.4 Sigmoidal Membership Function

A Sigmoidal membership function is defined by

$$f(x; a, c) = \frac{1}{1 + \exp[-a(x - c)]} \tag{4.5}$$

where a controls the slope at the crossover point $x = c$. Depending on the sign of the parameter , the Sigmoidal membership function is inherently open to the right or left, thus appropriate for representing the concepts such as "very large" or "very negative".

For example the sigmoidal membership function defined by sigmf (x, 2, 4) can be illustrated as shown in Figure 4.4.

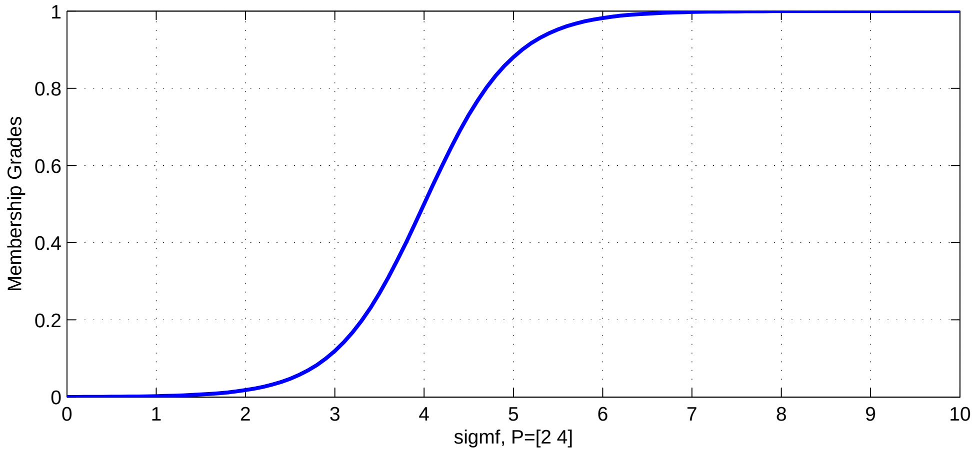

Figure 4.4: Sigmoidal Membership Function

4.3.5 Generalized bell Membership Function

A generalized bell membership function is specified by three parameters (a, b, c)

$$f(x; a, b, c) = \frac{1}{1 + \left|\frac{x-c}{a}\right|^{2b}} \tag{4.6}$$

where the parameter b is usually positive. The parameter c locates the centre of the curve. If b is negative, the slope of the membership function becomes an upside-down bell.

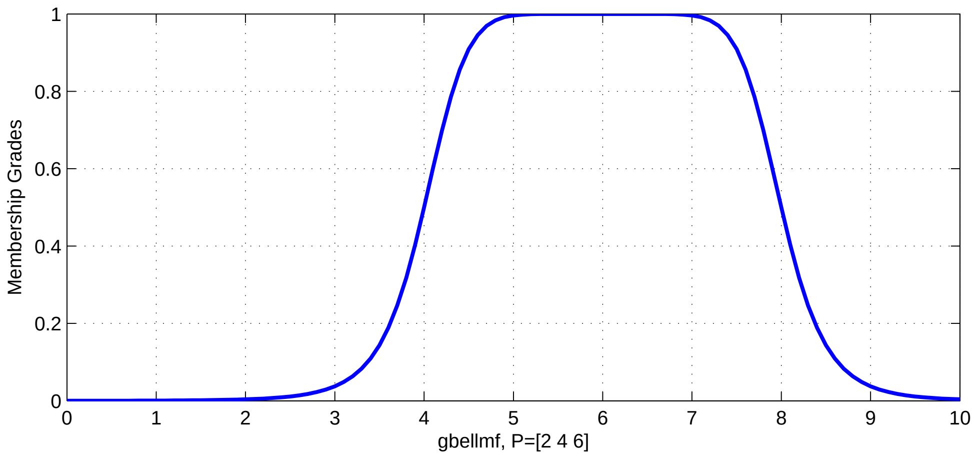

Figure 4.5: Generalized bell Membership Function

For example the generalized bell membership function defined by gbellmf (x, 2, 4, 6) can be illustrated as shown in Figure 4.5.

4.4 Fuzzy Systems

The fuzzy inference system or fuzzy system is a popular computing framework based on the concept of fuzzy set theory, fuzzy if-then rules, and fuzzy reasoning.

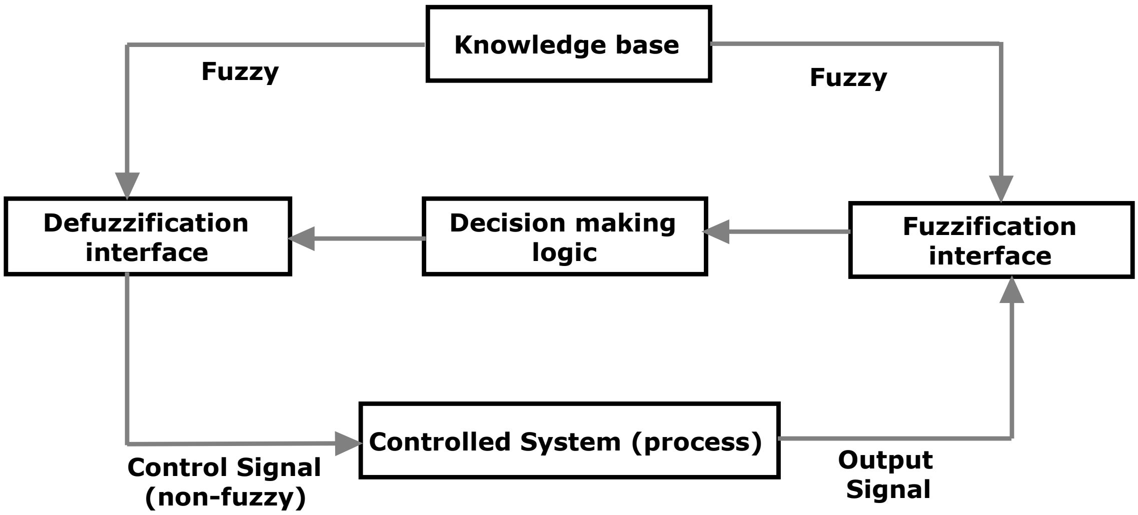

Figure 4.6: Block diagram of Fuzzy logic controller

The fuzzy inference system basically consists of a formulation of the mapping from a given input set to an output set using FL as shown in Figure 4.6. The mapping process provides the basis from which the inference or conclusion can be made. The basic structure of fuzzy inference system consists of three conceptual components: a rule base, which contains a selection of fuzzy rules; a data base, which defines the membership functions used in the fuzzy rules; and a reasoning mechanism which performs the inference procedure upon the rules and given facts to derive a reasonable output or conclusion.

The fuzzy logic controller comprises 4 principle components: fuzzification interface, knowledge base, decision making logic, and defuzzification interface.

- Fuzzification: In fuzzification, the values of input variables are measured i.e. it converts the input data into suitable linguistic values.
- Knowledge base: The knowledge base consists of a database and linguis-

tic control rule base. The database provides the necessary definitions, which are used to define the linguistic control rules and fuzzy data manipulation in an FLC. The rule base characterizes the control policy of domain experts by means of set of linguistic control rules.

- Decision making logic: The decision making logic has the capability of stimulating human decision making based on fuzzy concepts.
- Defuzzification: The defuzzification performs scale mapping, which converts the range of values of output variables into corresponding universe of discourse. If the output from the defuzzifier is a control action for a process, then the system is a non-fuzzy logic decision system. There are different techniques for defuzzification such as maximum method, height method, centroid method etc.

The basic inference process consists of the following five steps:

- Step 1: Fuzzification of input variables
- Step2: Application of fuzzy operator (AND, OR, NOT) in the IF (antecedent) part of the rule
- Step3: Implication from the antecedent to the consequent THEN part of the rule
- Step4: Aggregation of the consequents across the rules
- Step5: Defuzzification

4.5 Implication Methods

There are number of implication methods to fuzzy logic, but only two widely used methods are discussed here. Those are Mamdani type fuzzy model and Sugeno type fuzzy model.

4.5.1 Mamdani Fuzzy Model

Mamdani fuzzy rule for a fuzzy controller involving three input variables and two output variables can be described as follows:

IF x_1 is A AND x_2 is B AND x_3 is C THEN z_1 is D, z_2 is E.

where x_1, x_2, and x_3 are input variables (e.g., error, its first derivative and its second derivative), and z1 and z2 are output variables. In theory, these variables can be either continuous or discrete; practically speaking, they should be discrete because virtually all fuzzy controllers and models are implemented using digital computers. A, B, C, D and E are fuzzy sets. "IF x_1 is A AND x_2 is B AND x_3 is C" is called the rule antecedent, whereas the remaining part is named the rule consequent.

The structure of Mamdani fuzzy rules for fuzzy modeling is the same. The variables involved, however, are different. An example of a Mamdani fuzzy rule for fuzzy modeling is: IF y (t) is A AND y (t-1) is B AND y (t-2) is C AND u (t) is D AND u (t-1) is E THEN y (t+1) is F where A, B, C, D and E are fuzzy sets, y(t), y(t-1), and y(t-2) are the output of the system to be modeled at sampling time t, t-1 and t-2, respectively. And, u(t) and u(t-1) are system input at time t and t-1, respectively; y(t+1) is system output at the next sampling time, t+1.

Obviously, a general Mamdani fuzzy rule, for either fuzzy control or fuzzy modeling, can be expressed as: IF x_1 is A_1 AND x_2 is A_2 AND AND x_k is A_k THEN z_1 is B_1, z_2 is B_2 ..., z_m is B_m where x_i is the input variable, $i = 1, 2...k$ and z_i is the output variable, $j = 1, 2...m$. A_k is the input fuzzy set and B_m is the output fuzzy set.

4.5.2 Sugeno fuzzy model

The Sugeno fuzzy model or TSK fuzzy model was proposed by Takagi, Sugeno, and Kang and was introduced in 1985. A typical fuzzy rule in a Sugeno fuzzy model has the form

IF x is A and y is B then z = f (x, y), where A and B are fuzzy sets in the antecedent, while z = f (x, y) is a crisp function in the consequent. Usually z = f (x, y) is a polynomial in the input variables x and y, but it can be any function as long as it can appropriately describe the output of the model within the fuzzy region specified by the antecedent of the rule. When z = f (x, y) is a first-order polynomial, the resulting fuzzy inference system is called a first-order Sugeno fuzzy model. When f is a constant, we then have a zero-order Sugeno fuzzy model.

4.6 Defuzzification Methods

Defuzzification refers to the way a crisp value is extracted from a fuzzy set as a representative value. Several methods are available for Defuzzification. Here, a few of the widely used methods namely centroid method, centre of sums and mean of maximum are discussed.

4.6.1 Centroid Method

Centroid method is also known as centre of gravity method, it obtains the centre of area z^* occupied by the fuzzy set A of universe of discourse Z. It is given by the expression

$$z^* = \frac{\int_z \mu_A(z) z dz}{\int_z \mu_A(z) dz} \tag{4.7}$$

for a continuous membership function,

and

$$z^* = \frac{\sum_{i=1}^{n} z_i \mu(z_i)}{\sum_{i=1}^{n} \mu(z_i)} \tag{4.8}$$

for a discrete membership function.

where $\mu_A(z)$ is the aggregated output MF. This is the most widely used adopted Defuzzification strategy, which is reminiscent of the calculation of expected values of probability distributions.

4.6.2 Centre of Sums (COS) Method

In the centroid method, the overlapping area is counted once whereas in centre of sums, the overlapping area is counted twice. COS builds the resultant membership function by taking the algebraic sum of outputs from each of the contributing fuzzy sets A1, A2, A3,etc. The defuzzified value z^* is given by

$$z^* = \frac{\sum_{i=1}^{N} z_i \sum_{k=1}^{n} \mu_{A_k}(z_i)}{\sum_{i=1}^{N} \sum_{k=1}^{n} \mu_{A_k}(z_i)} \tag{4.9}$$

where n is the number of fuzzy sets and N is the number of fuzzy variables.

4.6.3 Mean of Maxima (MOM) Method

MOM is the average of the maximizing z^* at which the MF reach maximum μ^*. In symbols,

$$z^* = \frac{\sum_{z_i \varepsilon M} z_i}{|M|} \tag{4.10}$$

where M = $\{ z_i \mid \mu(z_i)$the height of the fuzzy set $\}$ and $|M|$ is the cardinality of the set M.

4.7 Design of Fuzzy Logic Based PSS

The basic structure of the fuzzy logic controller is shown in Figure 4.7. Here the inputs to the fuzzy logic controller are the normalized values of error 'e' and change of error 'ce'. Normalization is done to limit the universe of discourse of the inputs between -1 to 1 such that the controller can be successfully operated within a wide range of input variation. Here $'K_e'$ and $'K_{ce}'$ are the normalization factors for error input and change of error input respectively. For this fuzzy logic controller design, the normalization factors are taken as constants. The output of the fuzzy logic controller is then multiplied with a gain $'K_0'$ to give the appropriate control signal $'U'$. The output gain is also taken as a constant for this fuzzy logic controller.

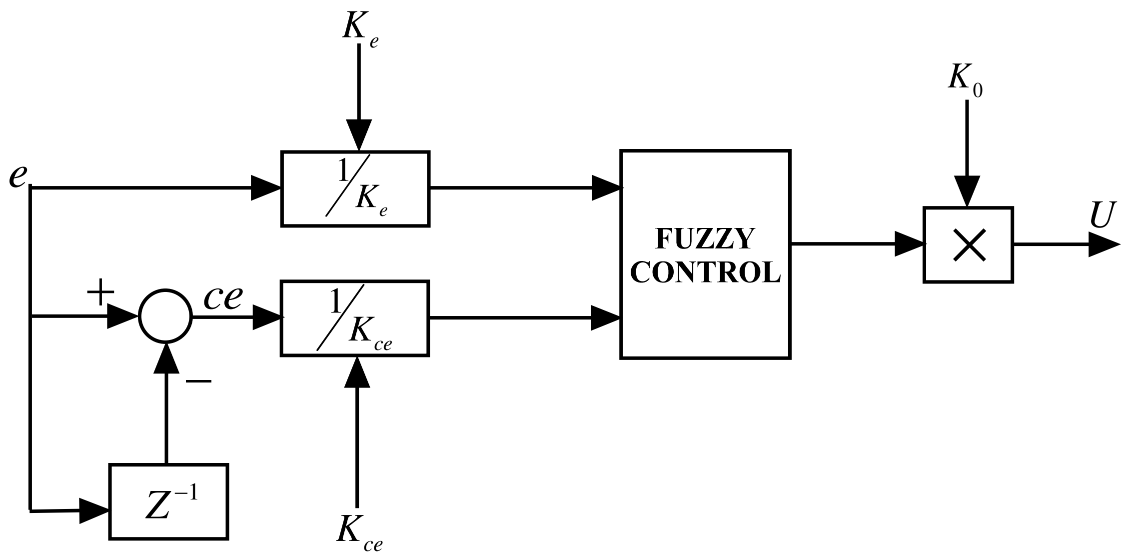

Figure 4.7: Basic Structure of Fuzzy Logic Controller

The fuzzy controller used in power system stabilizer is normally a two-input and a single-output component. It is usually a MISO system. The two inputs are change in angular speed and rate of change of angular speed whereas output of fuzzy logic controller is a voltage signal.

4.7.1 Input/output Variables

The design starts with assigning the mapped variables inputs/output of the fuzzy logic controller (FLC). The first input variable to the FLC is the generator speed deviation and the second is acceleration. The output variable to the FLC is the voltage.

After choosing proper variables as input and output of fuzzy controller, it is required to decide on the linguistic variables. These variables transform the numerical values of the input of the fuzzy controller to fuzzy quantities. The number of linguistic variables describing the fuzzy subsets of a variable varies according to the application. Here seven linguistic variables for each of the input and output variables are used to describe them. Table 4.1 shows the Membership functions for fuzzy variables.

The membership function maps the crisp values into fuzzy variables. The

NB	NEGATIVE BIG
NM	NEGATIVE MEDIUM
NS	NEGATIVE SMALL
ZE	ZERO
PS	POSITIVE SMALL
PM	POSITIVE MEDIUM
PB	POSITIVE BIG

Table 4.1: Membership functions for fuzzy variables

triangular membership functions are used to define the degree of membership. Here for each input variable, seven labels are defined namely, NB, NM, NS, ZE, PS, PM and PB. Each subset is associated with a triangular membership function to form a set of seven membership functions for each fuzzy variable.

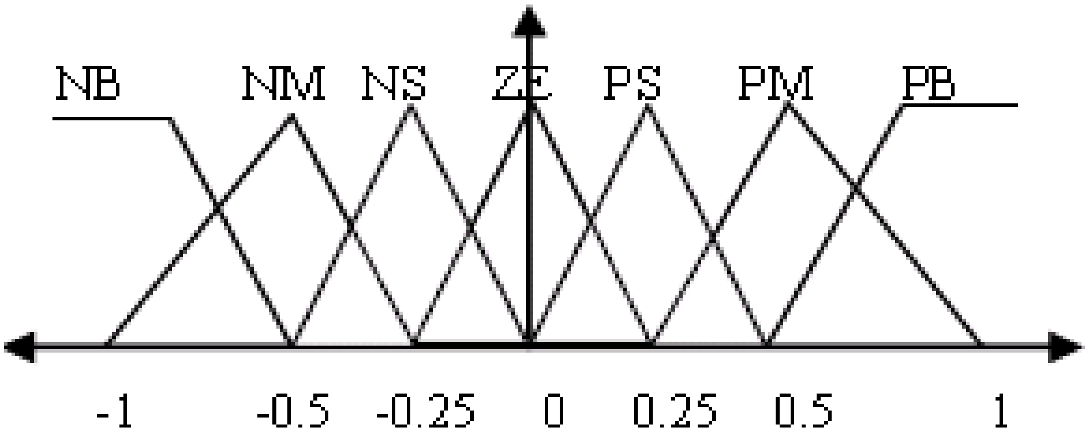

Figure 4.8: Membership function for speed deviation

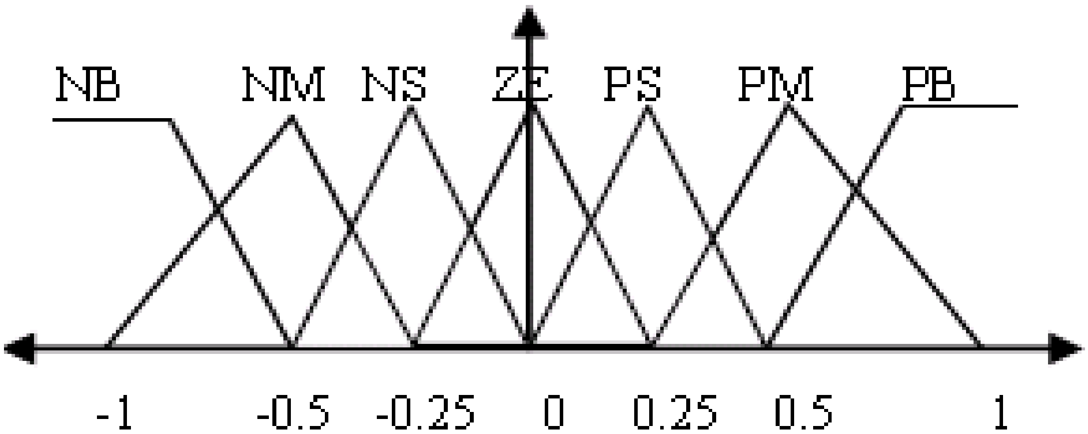

Figure 4.9: Membership function for acceleration

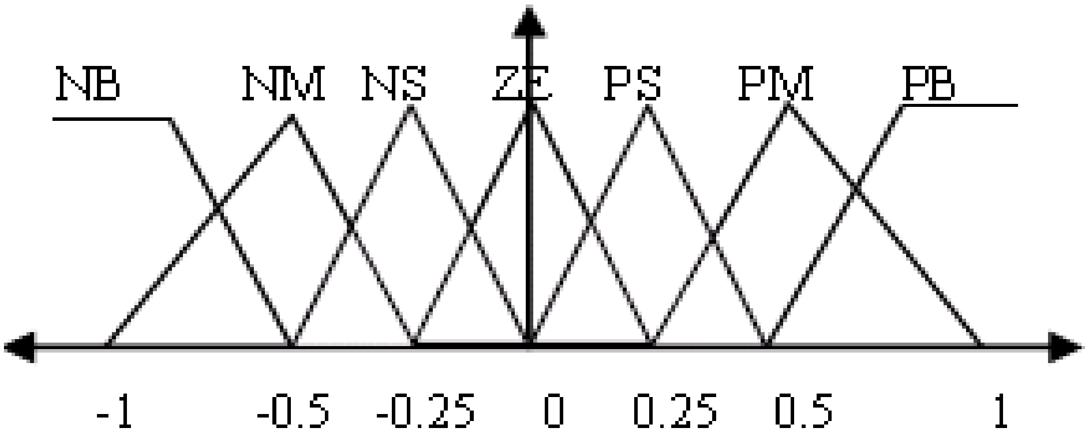

Figure 4.10: Membership function for voltage

Speed deviation \ acceleration	NB	NM	NS	ZE	PS	PM	PB
NB	NB	NB	NB	NS	ZE	ZE	PS
NM	NB	NB	NM	NS	ZE	PS	PM
NS	NB	NB	NM	ZE	PS	PM	PB
ZE	NB	NM	NS	ZE	PS	PM	PB
PS	NB	NM	NS	ZE	PM	PB	PB
PM	NM	NS	ZE	PS	PM	PB	PB
PB	NS	ZE	ZE	PS	PB	PB	PB

Table 4.2 Decision Table

The variables are normalized by multiplying with respective gains K_e,K_{ce},K_0 so that their values lie between -1 and +1. The membership function for speed deviation, acceleration and voltage are shown in Figure 4.8, Figure 4.9 and Figure 4.10 respectively.

Knowledge base involves defining the rules represented as IF - THEN rules statements governing the relationship between input and output variables in terms of membership functions. In this stage the input variables speed deviation and acceleration are processed by the inference engine that executes

7×7 rules represented in rule Table 4.2.

Each entity shown in Table 4.2 represent a rule. The antecedent of each rule conjuncts speed deviation ($\Delta\omega$) and acceleration (Δa) fuzzy set values.

The knowledge required to generate the fuzzy rules can be derived from an offline simulation. Some knowledge can be based on the understanding of the behavior of the dynamic system under control. For monotonic systems, a symmetrical rule table is very appropriate, although sometimes it may need slight adjustment based on the behavior of the specific system. If the system dynamics are not known or are highly nonlinear, trial and error procedures and experience play an important role in defining the rules.

An example of the rule is: If $\Delta\omega$ is NS and Δa is NM then U is NB which means that if the speed deviation is negative small and acceleration is negative medium then the output of fuzzy controller should be negative big.

The procedure for calculating the crisp output of the Fuzzy Logic Controller (FLC) for some values of input variables is based on the following three steps.

Step 1: Determination of degree of firing (DOF) of the rules

The DOF of the rule consequent is a scalar value which equals the minimum of two antecedent membership degrees. For example if $\Delta\omega$ is PS with a membership degree of 0.6 and Δa is PM with a membership degree of 0.4 then the degree of firing of this rule is 0.4.

Step2: Inference Mechanism

The inference mechanism consists of two processes called fuzzy implication and aggregation. The degree of firing of a rule interacts with its consequent to provide the output of the rule, which is a fuzzy subset. The formulation used to determine how the DOF and the consequent fuzzy set interact to form the rule output is called a fuzzy implication. In fuzzy logic control the most commonly used method for inferring the rule output is Mamdani method.

Step3: Defuzzification

To obtain a crisp output value from the fuzzy set obtained in the previous step a mechanism called defuzzification is used. In this example output U is defuzzified according to the membership functions shown in Figure 4.10. Here center of gravity (COA) or centroid method is used to calculate the final fuzzy value.

Defuzzification using COA method means that the crisp output of U is obtained by using the centre of gravity, in which the crisp U variable is taken to be the geometric centre of the output fuzzy variable value $\mu_{out}(U)$ area, where $\mu_{out}(U)$ is formed by taking the union of all the contributions of rules with the degree of fulfillment greater than zero. Then the COA expression with a discretized universe of discourse can be written as follows:

$$U^* = \frac{\sum_{k=1}^{n} U_k \mu_{out}(U_k)}{\sum_{k=1}^{n} \mu_{out}(U_k)} \tag{4.11}$$

Chapter 5

RESULTS AND DISCUSSION

5.1 The Case Study

In this chapter, simulation results using MATLAB / SIMULINK for both types of power system stabilizers (conventional and fuzzy based) are shown.

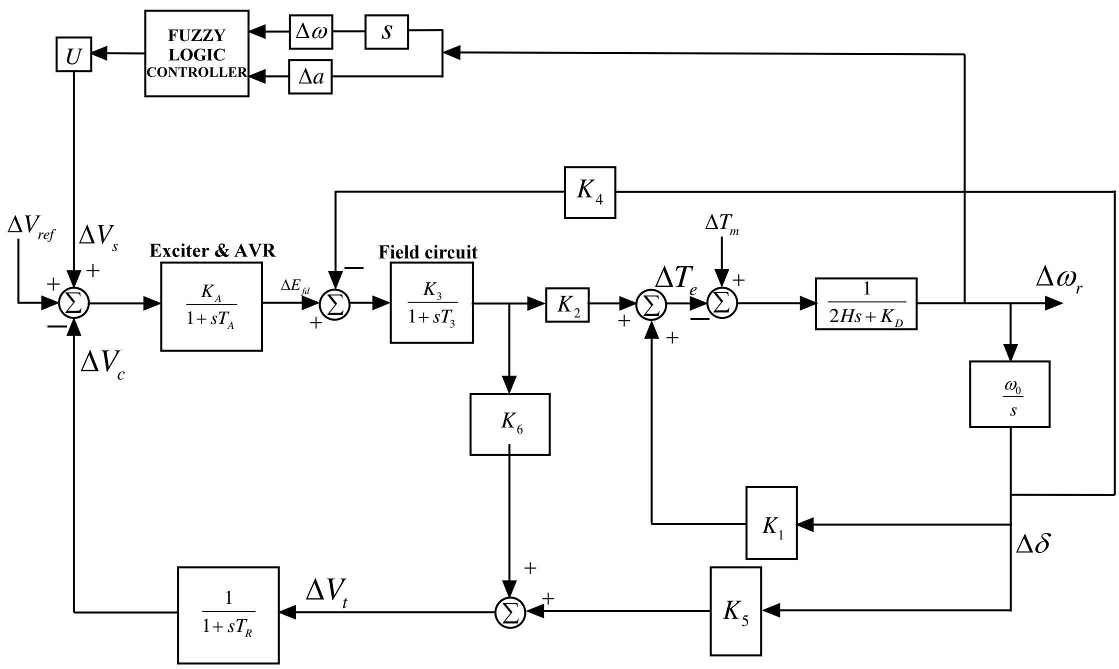

Figure 5.1: Test System for Proposed Fuzzy Logic Based PSS

The performance of the proposed model is tested on Single Machine Infinite Bus System (SMIB) as shown in Figure 5.1. Then the performance of SMIB system has been studied without excitation system, with excitation system only, with conventional PSS (lead-lag) and with fuzzy logic based PSS by using the K constants. The dynamic models of synchronous machine, excitation system, prime mover, governing system and conventional PSS are described in chapter 2.

5.2 Performance without Excitation System

In chapter 2, Figure 2.12 shows the block diagram representation with AVR and PSS. In this presentation, the dynamic characteristics of the system are expressed in terms of the so-called K - constants. The values of K - constants calculated using above parameters are

$K_1 = 1.7299$, $K_2 = 1.7325$, $K_3 = 0.1692$, $K_4 = 2.8543$, $K_5 = -0.0613$, $K_6 = 0.3954$

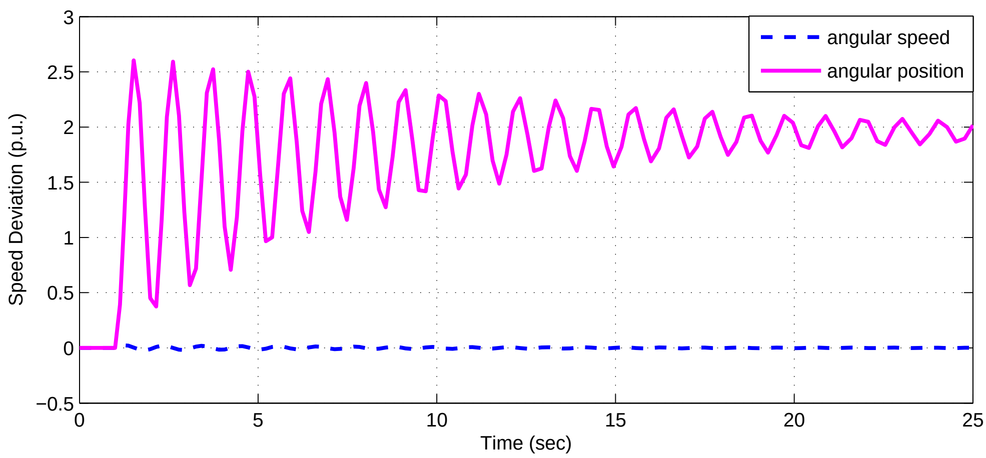

Figure 5.2: response without excitation system

Figure 5.2 shows the variation in angular speed and angular position. From the above response shown in Figure 5.2 it shows that it is taking very large time i.e. more than 25 seconds to settle to steady state. Therefore, the performance of the system with excitation system is analyzed to find the suitability of the excitation system in removing these oscillations.

5.3 Performance with Excitation System

The time response of the angular speed and angular position with excitation system has shown in Figure 5.3 and Figure 5.4 for positive and negative value of K_5 constant.

From Figure 5.3 the response characteristic shows that under damped oscillations are resulted. The figure shows that it has negative damping due to the fact that K_5 constant calculated above is negative, which is true for high values for external system reactance and high generator outputs.

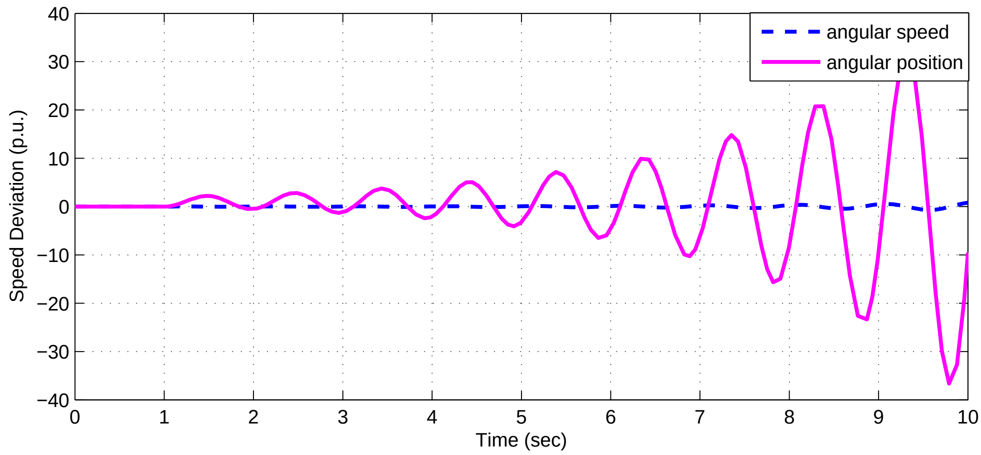

Figure 5.3: Response with excitation system for -ve K_5

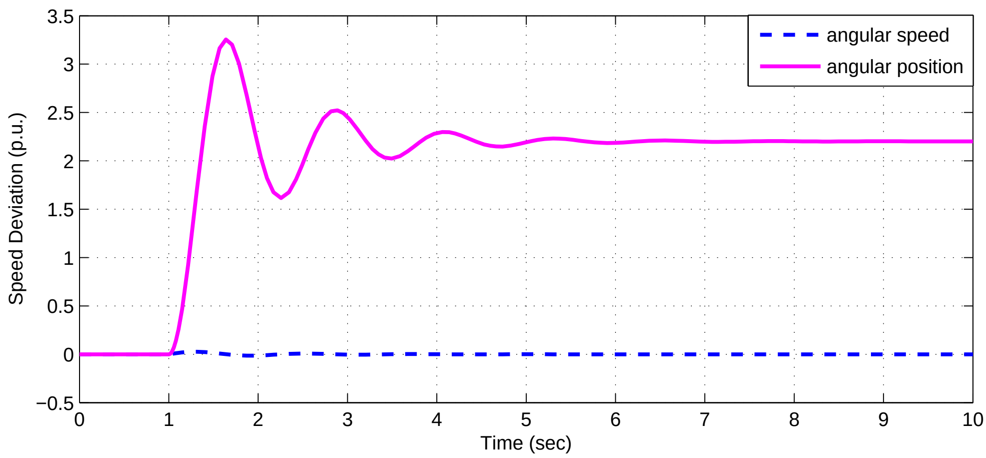

Figure 5.4: Response with excitation system for +ve K_5

The performance when analyzed with positive value of K_5, the system is stable. Positive K_5 is possible for low values of external system reactance and low generator outputs. So for positive the damping is positive and thus the system is stable.

5.4 Performance with Conventional PSS

Figure 5.5 shows the variation of angular speed and angular position when PSS (lead-lag) is applied for negative value of K_5.

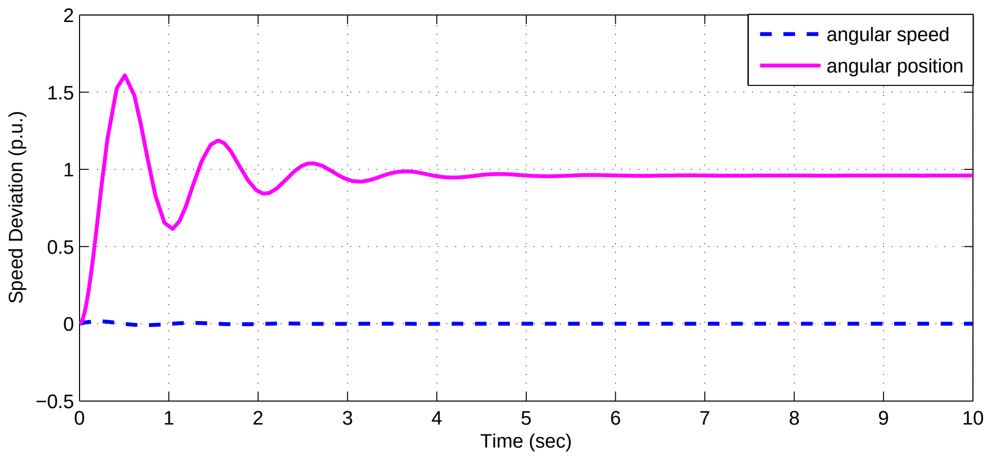

Figure 5.5: Response with CPSS for -ve K_5

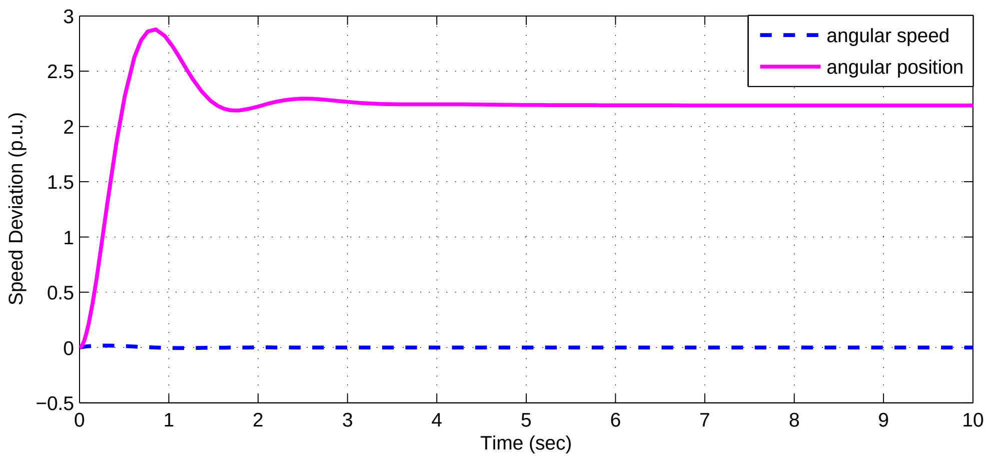

Figure 5.6: Response with CPSS for +ve K_5

From the Figure 5.5 and Figure 5.6 it shows that the system is stable for both positive and negative value of K_5 constant. The transients are more for negative K_5 whereas higher angular position is attained with positive K_5.

5.5 Performance with Fuzzy Logic Based PSS

The model used in Simulink/Matlab to analyze the effect of fuzzy logic controller in damping small signal oscillations when implemented on single machine infinite bus system is shown in Figure 5.1.

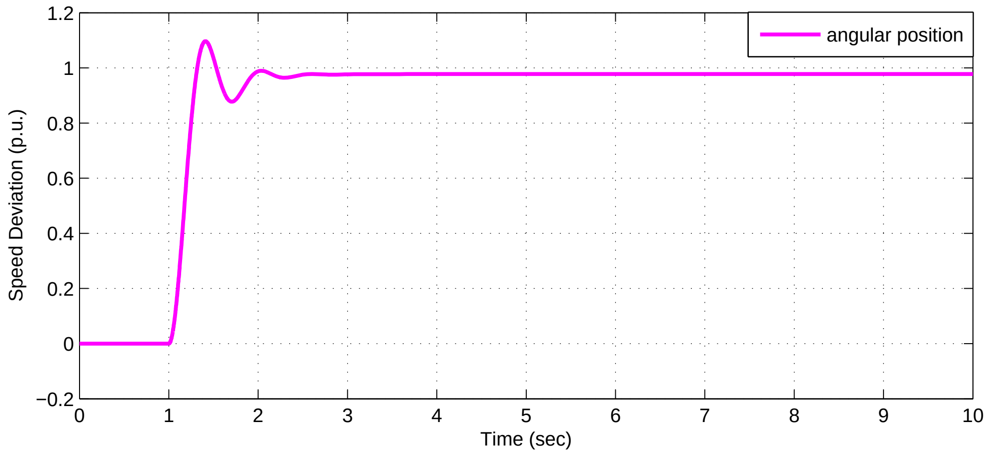

Figure 5.7: Variation of angular position with FLPSS for -ve K_5

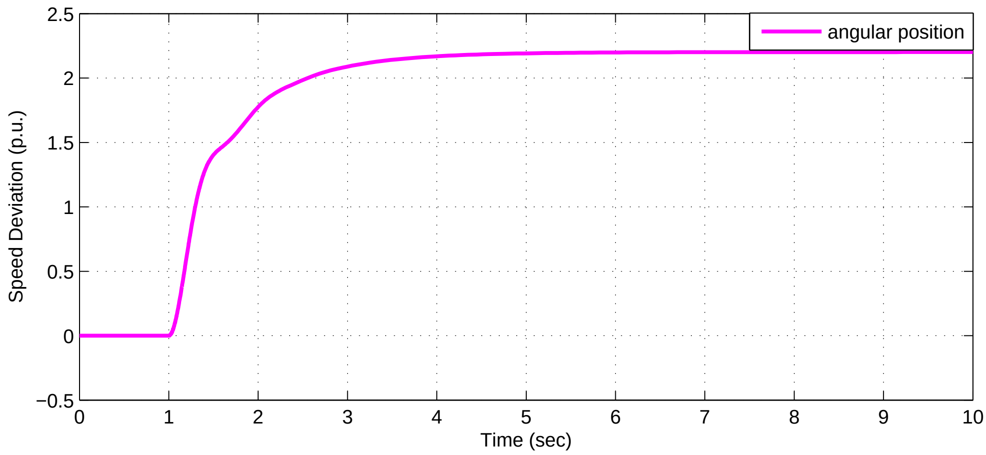

Figure 5.8: Variation of angular position with FLPSS for +ve K_5

The variation of angular position with fuzzy logic based PSS for negative and positive value of K_5 constant is shown in Figure 5.7 and Figure 5.8 respectively.

The variation of angular speed with fuzzy logic based PSS for negative and positive value of K_5 constant is shown in Figure 5.9 and Figure 5.10

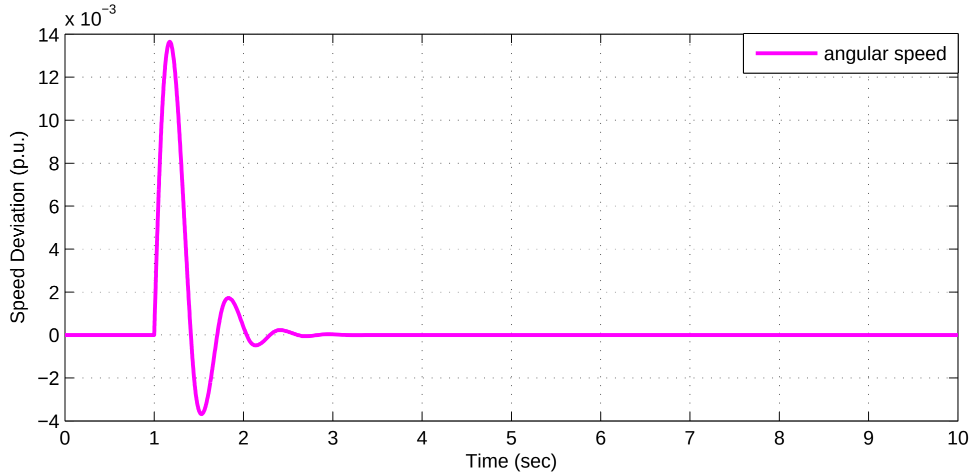

Figure 5.9: Variation of angular speed with FLPSS for -ve K_5

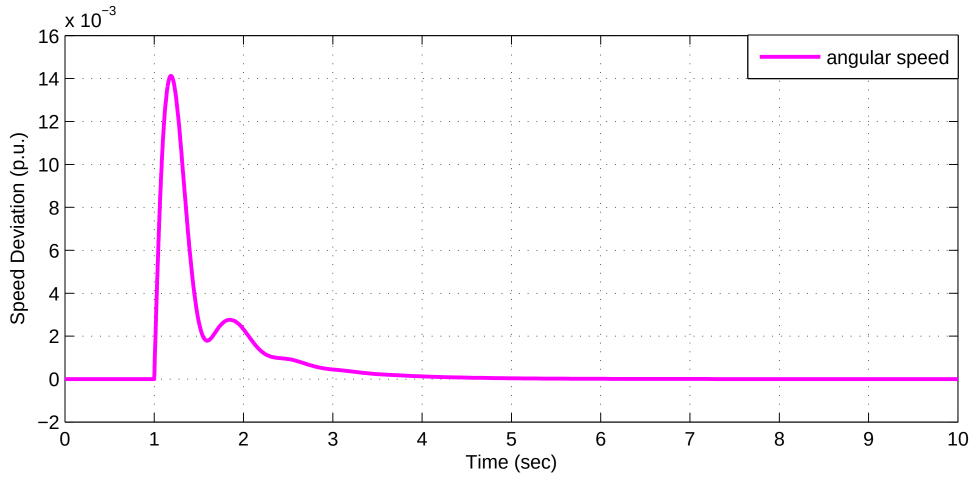

Figure 5.10: Variation of angular speed with FLPSS for +ve K_5

respectively. Figure 5.7 and Figure 5.9 show that the angular position and angular speed stabilizes to a particular value with very few oscillations for negative value of K_5constant. For positive value of K_5 constant angular position attains higher value than conventional PSS.

5.6 Performance with different membership functions

Figure 5.11 and Figure 5.12 show the angular position and angular speed of different membership function (Gaussian, Trapezoidal and Triangular) for positive value of K_5 constant respectively. As shown in Figure 5.11 and Figure 5.12, the oscillations are more pronounced in case of inputs and outputs

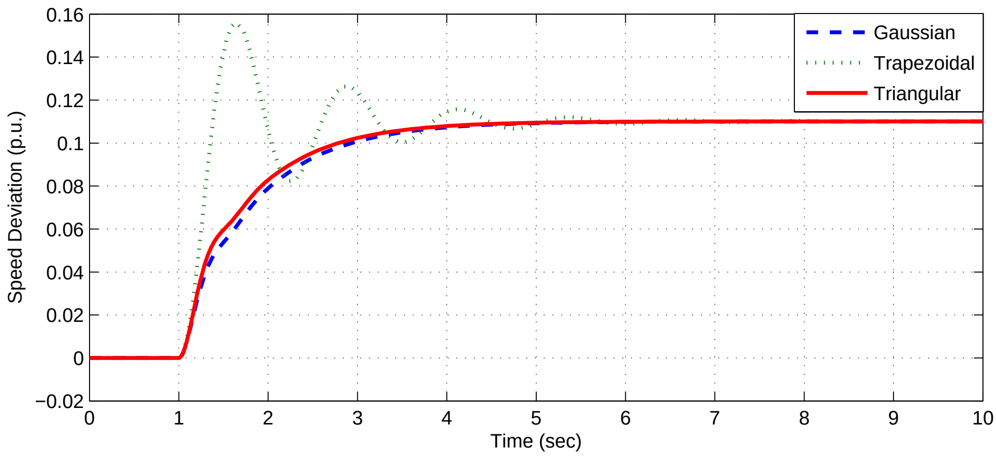

Figure 5.11: Angular position of different membership function for +ve K_5

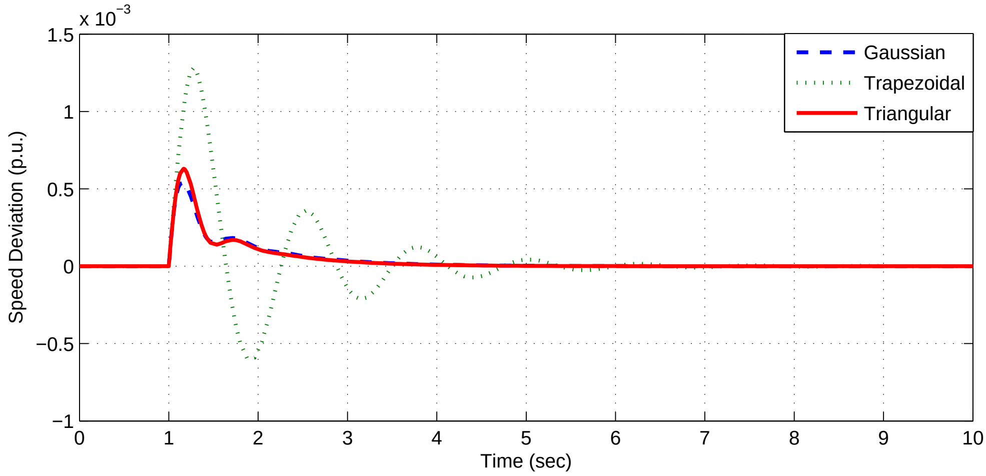

Figure 5.12: Angular speed of different membership function for +ve K_5

having trapezoidal membership functions for positive value of K_5 and the system becomes stable after a long time of 8.2 second approximately.

Figure 5.13 and Figure 5.14 show the angular position and angular speed of different membership function (Gaussian, Trapezoidal and Triangular) for negative value of K_5 constant respectively. As shown in Figure 5.13 and Figure 5.14, the unstable behavior is resulted if the trapezoidal membership function is used with negative value of K_5 constant. The performance using gaussian and triangular membership functions is comparable and the system becomes stable after in nearly 3 second.

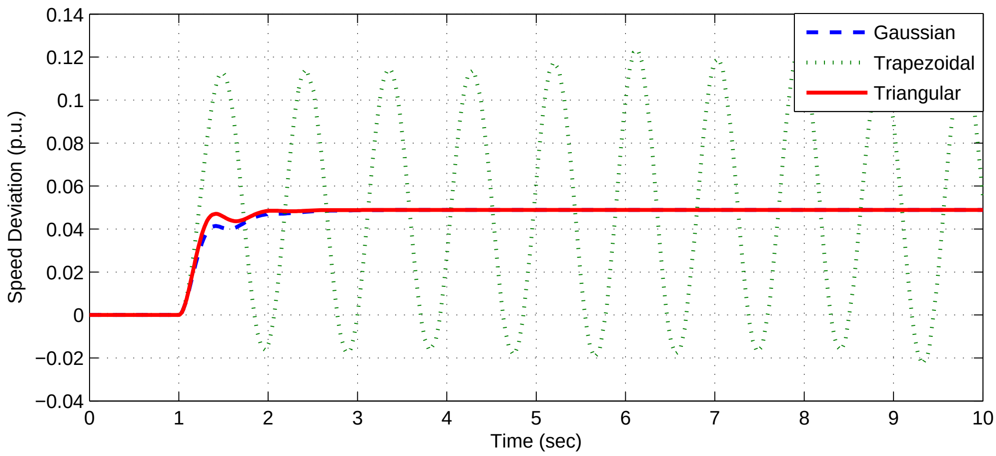

Figure 5.13: Angular position of different membership function for -ve K_5

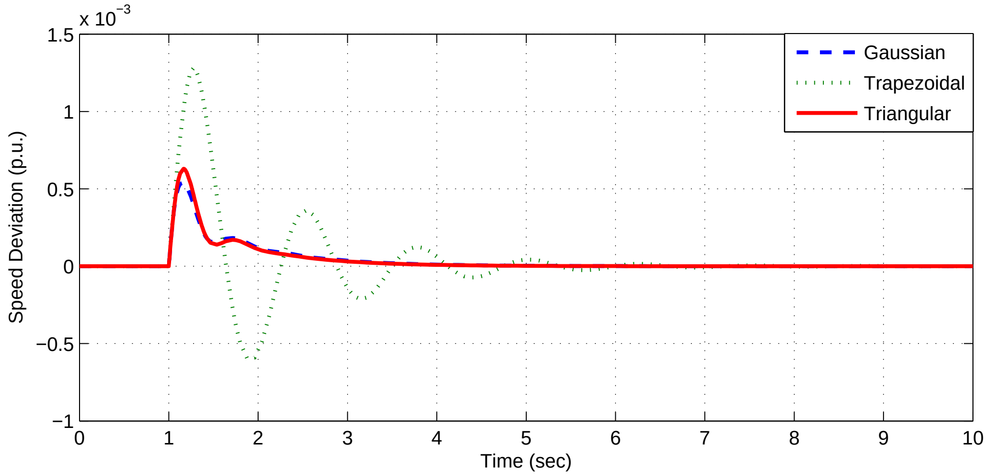

Figure 5.14: Angular speed of different membership function for -ve K_5

5.7 Response for different operating conditions using Triangular MF

Figure 5.15 and Figure 5.16 show the angular position at different operating conditions for negative and positive value of K_5 constant respectively.

Figure 5.17 and Figure 5.18 show the angular speed at different operating conditions for negative and positive value of K_5 constant respectively.

Figure 5.15, Figure 5.16, Figure 5.17 and Figure 5.18 shows the response for different operating conditions using triangular membership functions and the result shows that the response is coming out to the stable state with very few oscillations thus enhancing the stability of a system.

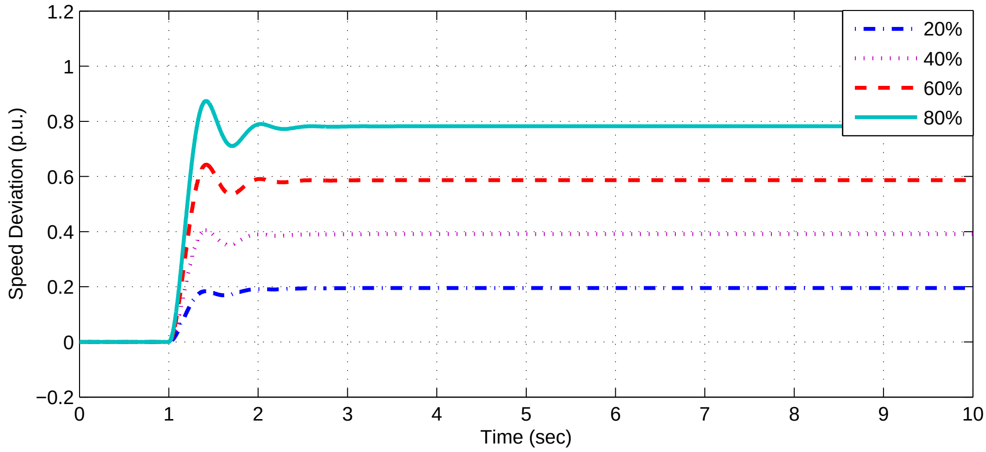

Figure 5.15: Angular position for different operating conditions for -ve K_5

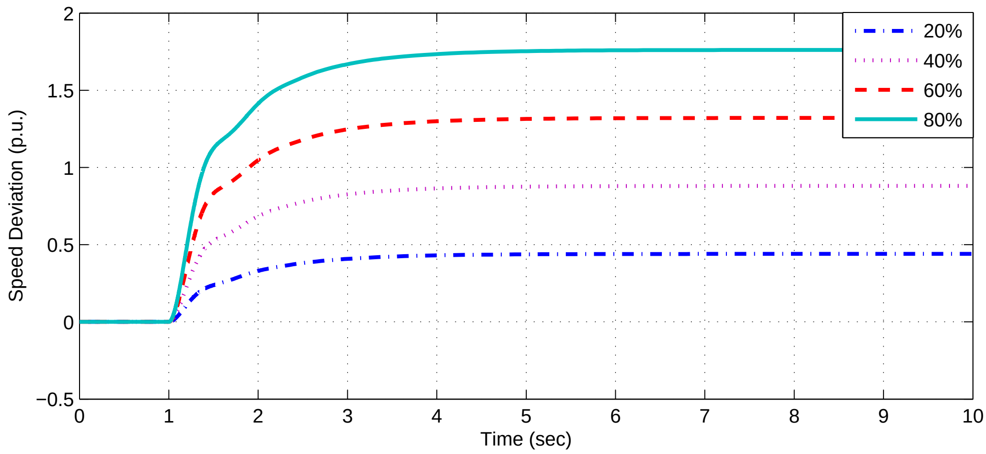

Figure 5.16: Angular position for different operating conditions for +ve K_5

5.8 Comparison of Conventional PSS and Fuzzy Logic Based PSS

Figure 5.19 shows the variation of angular position with conventional PSS and fuzzy logic based PSS for negative value of K_5.

Figure 5.20 shows the variation of angular position with conventional PSS and fuzzy logic based PSS for positive value of K_5.

Figure 5.21 shows the variation of angular speed with conventional PSS and fuzzy logic based PSS for negative value of K_5.

Figure 5.22 shows the variation of angular speed with conventional PSS and fuzzy logic based PSS for positive value of K_5.

From Figure 5.19 and Figure 5.21 it depicts that the system reaches its

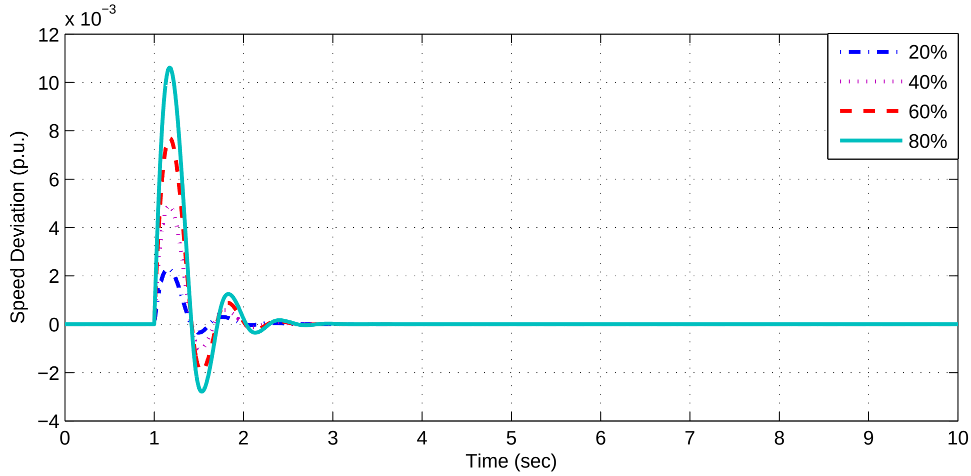

Figure 5.17: Angular speed for different operating conditions for -ve K_5

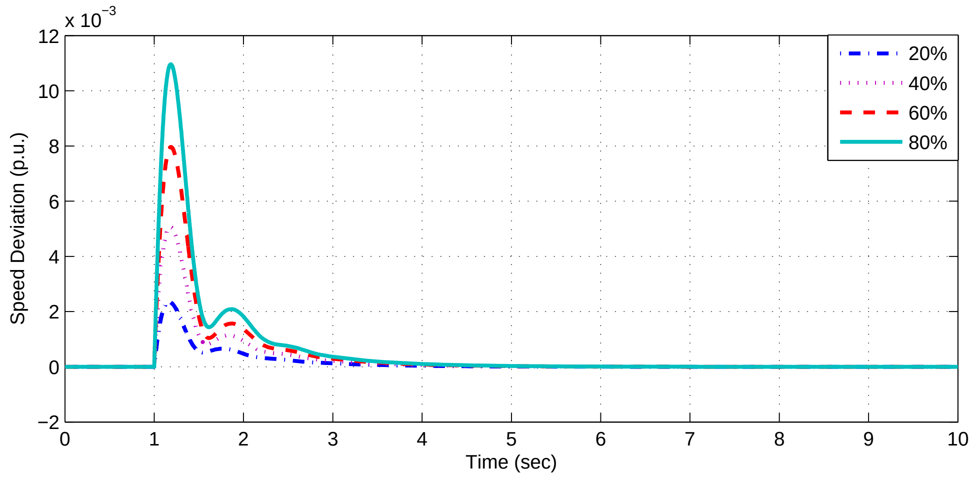

Figure 5.18: Angular speed for different operating conditions for +ve K_5

steady state value much earlier with FuzzyPSS compared to conventional PSS for negative value of K_5 constant.

From Figure 5.20 and Figure 5.22 it is seen that the sluggish response or over damped response characteristic is resulted and the settling time remains largely unchanged for positive value of K_5 constant.

From Figure 5.21 and Figure 5.22 it shows that oscillations in angular speed reduces much faster with fuzzy logic based PSS (FLPSS) than with conventional PSS (CPSS) for both cases i.e. for positive and negative value of K_5 constant.

As shown in Figure 5.21 with fuzzy logic based PSS (FLPSS), the variation

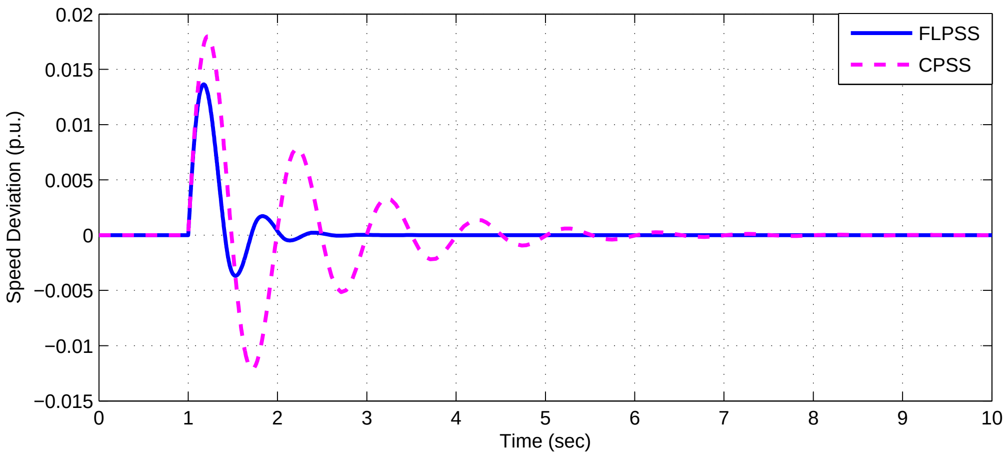

Figure 5.19: Comparison of angular position between CPSS and FLPSS for -ve K_5

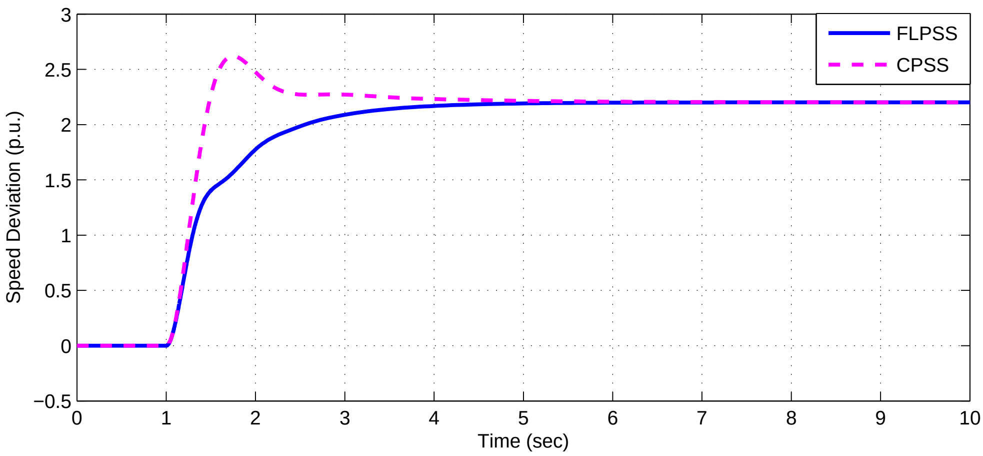

Figure 5.20: Comparison of angular position between CPSS and FLPSS for +ve K_5

in angular speed reduces to zero in about 2 to 3 seconds but with conventional PSS (CPSS), it takes about 6 seconds to reach to the final steady state value and also the oscillations are less pronounced in FLPSS.

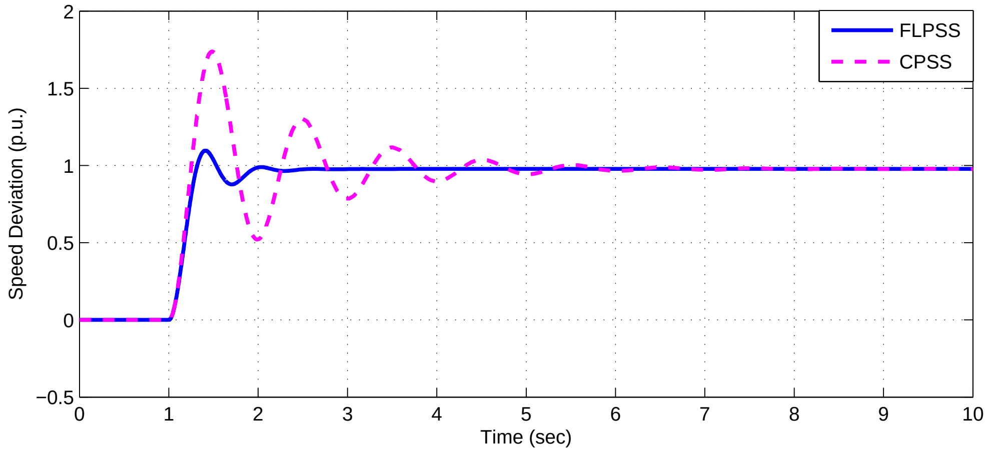

Figure 5.21: Comparison of angular speed between CPSS and FLPSS for -ve K_5

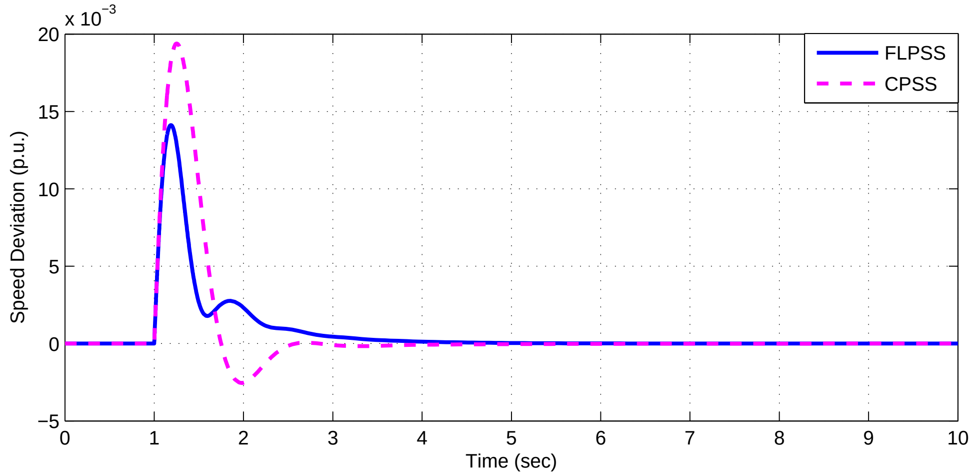

Figure 5.22: Comparison of angular speed between CPSS and FLPSS for +ve K_5

Chapter 6

CONCLUSION AND SUGGESTIONS FOR FUTURE WORK

6.1 Conclusion

In this thesis work initially the effectiveness of power system stabilizer in damping power system stabilizer is reviewed. Then the fuzzy logic based power system stabilizer is introduced by taking speed deviation and acceleration of synchronous generator as the input signals to the fuzzy controller and voltage as the output signal. FLPSS shows the better control performance than power system stabilizer in terms of settling time and damping effect. Therefore, it can be concluded that the performance of FLPSS is better than conventional PSS. However, the choice of membership functions has an important bearing on the damping of oscillations. From the simulation studies it shows that the oscillations are more pronounced in case of trapezoidal membership functions. The response with gaussian membership functions is comparable to triangular membership functions. However, the performance of FLPSS with triangular membership functions is superior compared to other membership functions.

6.2 Suggestions for future work

Having gone through the study of fuzzy logic based PSS (FLPSS) for single machine infinite bus system, the scope of the work is

1. The fuzzy logic based PSS (FLPSS) can be extended to multi machine interconnected system having non-linear industrial loads which may introduce phase shift.
2. The fuzzy logic based PSS with frequency as input parameter can be investigated because the frequency is highly sensitive in weak system, which may offset the controller action on the electrical torque of the machine.
3. Testing using more complex network models can be carried out.

Bibliography

[1] T. Abdelazim and O. Malik, "An adaptive power system stabilizer using on-line self-learning fuzzy systems," in *Power Engineering Society General Meeting, 2003, IEEE*, vol. 3, july 2003, pp. 1715 – 1720 Vol. 3.

[2] A. Al-Hinai, "Dynamic stability enhancement using genetic algorithm power system stabilizer," in *Power System Technology (POWERCON), 2010 International Conference on*, oct. 2010, pp. 1 –7.

[3] K. Al-Olimat, A. Farhoud, and J. Hurtig, "Power system stabilizers with fuzzy logic switching," in *Power Systems Conference and Exposition, 2006. PSCE '06. 2006 IEEE PES*, 29 2006-nov. 1 2006, pp. 2152 –2157.

[4] P. M. Anderson, A. A. Fouad, and H. H. Happ, "Power system control and stability," *Systems, Man and Cybernetics, IEEE Transactions on*, vol. 9, no. 2, p. 103, feb. 1979.

[5] A. Babaei, S. Razavi, S. Kamali, and A. Gholami, "Performance improvement of power system stabilizer by genetic algorithm for one machine infinite bus system," in *Universities Power Engineering Conference, 2007. UPEC 2007. 42nd International*, sept. 2007, pp. 344 –348.

[6] M. Basler and R. Schaefer, "Understanding power system stability," in *Protective Relay Engineers, 2005 58th Annual Conference for*, april 2005, pp. 46 – 67.

[7] H. Behbehani, J. Bialek, and Z. Lubosny, "Enhancement of power system stability using fuzzy logic based supervisory power system stabilizer," in *Power and Energy Conference, 2008. PECon 2008. IEEE 2nd International*, dec. 2008, pp. 479 –484.

[8] W.-C. Chan and Y.-Y. Hsu, "An optimal variable structure stabilizer for power system stabilization," *Power Apparatus and Systems, IEEE Transactions on*, vol. PAS-102, no. 6, pp. 1738 –1746, june 1983.

[9] A. Chatterjee, S. Ghoshal, and V. Mukherjee, "A comparative study of single input and dual input power system stabilizer by hybrid evolutionary programming," in *Nature Biologically Inspired Computing, 2009. NaBIC 2009. World Congress on*, dec. 2009, pp. 1047 –1052.

[10] D. Chaturvedi, O. Malik, and P. Kalra, "Experimental studies with a generalized neuron-based power system stabilizer," *Power Systems, IEEE Transactions on*, vol. 19, no. 3, pp. 1445 – 1453, aug. 2004.

[11] C.-J. Chen, T.-C. Chen, H.-J. Ho, and C.-C. Ou, "Pss design using adaptive recurrent neural network controller," in *Natural Computation, 2009. ICNC '09. Fifth International Conference on*, vol. 2, aug. 2009, pp. 277 –281.

[12] W. Chi-Jui and H. Yuan-Yih, "Design of self-tuning pid power system stabilizer for multimachine power systems," *Power Systems, IEEE Transactions on*, vol. 3, no. 3, pp. 1059 –1064, aug 1988.

[13] J. H. Chow and J. J. Sanchez-Gasca, "Pole-placement designs of power system stabilizers," *Power Engineering Review, IEEE*, vol. 9, no. 2, pp. 60 –61, feb. 1989.

[14] J. Chow, G. Boukarim, and A. Murdoch, "Power system stabilizers as undergraduate control design projects," *Power Systems, IEEE Transactions on*, vol. 19, no. 1, pp. 144 – 151, feb. 2004.

[15] F. Demello and C. Concordia, "Concepts of synchronous machine stability as affected by excitation control," *Power Apparatus and Systems, IEEE Transactions on*, vol. PAS-88, no. 4, pp. 316 –329, april 1969.

[16] T. L. DeMello F.P., P.J. Nolan and J. Undrill, "coordinated application of stabilizers in multi machine power system," *Proceedings of the Twenty-First Annual North-American Power Symposium*, vol. Issue, 9-10, pp. 175 – 184., july 1989.

[17] M. Dobrescu and I. Kamwa, "A new fuzzy logic power system stabilizer performances," in *Power Systems Conference and Exposition, 2004. IEEE PES*, oct. 2004, pp. 1056 – 1061 vol.2.

[18] A. Dysko, W. Leithead, and J. O'Reilly, "Enhanced power system stability by coordinated pss design," *Power Systems, IEEE Transactions on*, vol. 25, no. 1, pp. 413 –422, feb. 2010.

[19] R. Gupta, B. Bandyopadhyay, and A. Kulkarni, "Design of power system stabiliser for single-machine system using robust periodic output feedback controller," *Generation, Transmission and Distribution, IEE Proceedings-*, vol. 150, no. 2, pp. 211 – 216, march 2003.

[20] R. Gupta, D. Sambariya, and R. Gunjan, "Fuzzy logic based robust power system stabilizer for multi-machine power system," in *Industrial Technology, 2006. ICIT 2006. IEEE International Conference on*, dec. 2006, pp. 1037 –1042.

[21] S. Gupta, N; Jain, "Comparative analysis of fuzzy power system stabilizer using different membership functions,," *International Journal of Computer and Electrical Engineering*, vol. 2, no. 2, april. 2010.

[22] G. Gurrala and I. Sen, "A modified heffron-phillip's model for the design of power system stabilizers," in *Power System Technology and IEEE Power India Conference, 2008. POWERCON 2008. Joint International Conference on*, oct. 2008, pp. 1 –6.

[23] ——, "Power system stabilizers design for interconnected power systems," *Power Systems, IEEE Transactions on*, vol. 25, no. 2, pp. 1042 –1051, may 2010.

[24] T. Hussein, A. Elshafei, and A. Bahgat, "Design of a hierarchical fuzzy logic pss for a multi-machine power system," in *Control Automation, 2007. MED '07. Mediterranean Conference on*, june 2007, pp. 1 –6.

[25] T. Hussein, M. Saad, A. Elshafei, and A. Bahgat, "Damping inter-area modes of oscillation using an adaptive fuzzy power system stabilizer," in *Control and Automation, 2008 16th Mediterranean Conference on*, june 2008, pp. 368 –373.

[26] G.-H. Hwang, J.-H. Park, H. T. Kang, and S. Kim, "Design of fuzzy power system stabilizer using adaptive evolutionary algorithm," in *Industrial Electronics, 2000. ISIE 2000. Proceedings of the 2000 IEEE International Symposium on*, vol. 1, 2000, pp. 42 –47 vol.1.

[27] A. Jalilvand, R. Aghmasheh, and E. Khalkhali, "Robust design of pid power system stabilizer in multi-machine power system using artificial intelligence techniques," in *Power Engineering and Optimization Conference (PEOCO), 2010 4th International*, june 2010, pp. 38 –42.

[28] S. Kamalasadan and G. Swann, "A novel power system stabilizer based on fuzzy model reference adaptive controller," in *Power Energy Society General Meeting, 2009. PES '09. IEEE*, july 2009, pp. 1 –8.

[29] M. Kothari and T. Kumar, "A new approach for designing fuzzy logic power system stabilizer," in *Power Engineering Conference, 2007. IPEC 2007. International*, dec. 2007, pp. 419 –424.

[30] P. Kundur., "Power system control and stability," *New York: McGraw-Hill*, vol. PAS-88, pp. 1103–1166, 1994.

[31] E. Larsen and D. Swann, "Applying power system stabilizers part i, ii, iii: Practical considerations," *Power Apparatus and Systems, IEEE Transactions on*, vol. PAS-100, no. 6, pp. 3034 –3046, june 1981.

[32] Y. Lin, "Systematic approach for the design of a fuzzy power system stabiliser," in *Power System Technology, 2004. PowerCon 2004. 2004 International Conference on*, vol. 1, nov. 2004, pp. 747 – 752 Vol.1.

[33] J. Lu, M. Nehrir, and D. Pierre, "A fuzzy logic-based adaptive power system stabilizer for multi-machine systems," in *Power Engineering Society Summer Meeting, 2000. IEEE*, vol. 1, 2000, pp. 111 –115 vol. 1.

[34] M. M. M. F. Othman and D. Linkens, "Designing power system stabilizer for multi machine power system using neuro-fuzzy algorithm," *jurnal Teknologi*, pp. 55–64, 2001.

[35] F. M. H. M. Saidy, "Performance improvement of a conventional power system stabilizer," *International Journal of Electrical Power and Energy Systems*, vol. 150, no. 5, pp. 313–323, oct. 2005.

[36] J. Matsuki, T. Okada, and K. Sakurai, "Experimental approach to optimal setting of parameters in fuzzy control algorithm for power system stabilization," in *Industrial Electronics, Control, and Instrumentation, 1993. Proceedings of the IECON '93., International Conference on*, nov 1993, pp. 273 –278 vol.1.

[37] N. Nallathambi and P. Neelakantan, "Fuzzy logic based power system stabilizer," in *E-Tech 2004*, july 2004, pp. 68 – 73.

[38] K. R. Padiyar, "Power system dynamics: Stability and control," in *printed in the Republic of Singapore, ISBN: 0-471-19002-0*, 1996.

[39] Y.-M. Park, U.-C. Moon, and K. Lee, "A self-organizing power system stabilizer using fuzzy auto-regressive moving average (farma) model," *Energy Conversion, IEEE Transactions on*, vol. 11, no. 2, pp. 442 –448, jun 1996.

[40] G. Radman and Y. Smaili, "Performance evaluation of pid power system stabilizer for synchronous generator," in *Southeastcon '88., IEEE Conference Proceedings*, apr 1988, pp. 597 –601.

[41] M. Ramirez-Gonzalez and O. Malik, "Simplified fuzzy logic controller and its application as a power system stabilizer," in *Intelligent System Applications to Power Systems, 2009. ISAP '09. 15th International Conference on*, nov. 2009, pp. 1 –6.

[42] F. Rashidi, M. Rashidi, and H. Amiri, "An adaptive fuzzy sliding mode control for power system stabilizer," in *Industrial Electronics Society, 2003. IECON '03. The 29th Annual Conference of the IEEE*, vol. 1, nov. 2003, pp. 626 – 630 vol.1.

[43] G. Rogers, "Demystifying power system oscillations," *Computer Applications in Power, IEEE*, vol. 9, no. 3, pp. 30 –35, jul 1996.

[44] A. Roosta, H. Khorsand, and M. Nayeripour, "Design and analysis of fuzzy power system stabilizer," in *Innovative Smart Grid Technologies Conference Europe (ISGT Europe), 2010 IEEE PES*, oct. 2010, pp. 1 –7.

[45] A. Singh and I. Sen, "A novel fuzzy logic based power system stabilizer for a multimachine system," in *TENCON 2003. Conference on Convergent Technologies for Asia-Pacific Region*, vol. 3, oct. 2003, pp. 1002 – 1006 Vol.3.

[46] D. Sumina, N. Bulic, and G. Erceg, "Simulation model of neural network based synchronous generator excitation control," in *Power Electronics and Motion Control Conference, 2008. EPE-PEMC 2008. 13th*, sept. 2008, pp. 556 –560.

[47] A. E. T. Hussein, M.S. Saad and A. Bahgat, "Robust adaptive fuzzy logic power system stabilizer," *An International Journal*, vol. 36, no. 10, dec. 2009.

[48] A. Taher, S.A.; Shemshadi, "Design of robust fuzzy logic power system stabilizer," *World Academy of Science, Engineering and Technology*, no. 27, 2007.

[49] H. Toliyat, J. Sadeh, and R. Ghazi, "Design of augmented fuzzy logic power system stabilizers to enhance power systems stability," *Energy Conversion, IEEE Transactions on*, vol. 11, no. 1, pp. 97 –103, mar 1996.

[50] J. Van Ness, F. Brasch, G. Landgren, and S. Naumann, "Analytical investigation of dynamic instability occuring at powerton station," *Power Apparatus and Systems, IEEE Transactions on*, vol. PAS-99, no. 4, pp. 1386 –1395, july 1980.

[51] M. Vani, G. Raju, and K. Prasad, "Robust supplementary controllers for avr and pss," in *India Conference (INDICON), 2009 Annual IEEE*, dec. 2009, pp. 1 –4.

[52] C. Vournas and J. Mantzaris, "Application of qss modeling to stabilizer design for interarea oscillations," *Power Systems, IEEE Transactions on*, vol. 25, no. 4, pp. 1910 –1917, nov. 2010.

[53] W. Watson and G. Manchur, "Experience with supplementary damping signals for generator static excitation systems," *Power Apparatus and Systems, IEEE Transactions on*, vol. PAS-92, no. 1, pp. 199 –203, jan. 1973.

[54] S. K. Yee and J. Milanovic, "Fuzzy logic controller for decentralized stabilization of multimachine power systems," *Fuzzy Systems, IEEE Transactions on*, vol. 16, no. 4, pp. 971 –981, aug. 2008.

[55] Y.-N. Yu and Q.-H. Li, "Pole-placement power system stabilizers design of an unstable nine-machine system," *Power Systems, IEEE Transactions on*, vol. 5, no. 2, pp. 353 –358, may 1990.

Appendices

Appendix A

System Data

The Parameters of the synchronous machine, excitation system and conventional PSS are as follows.

[a] Synchronous machine constants: x_d= 2.64 pu, $x_d^{'}$= 0.28 pu
x_q= 1.32 pu, $x_q^{'}$= 0.29 pu
R_E= 0.004 pu, X_E= 0.73 pu
f= 60 Hz, H= 4.5 sec

[b] Excitation system constants: K_A= 100, T_A= 0.05, T_R= 0.015
E_{FMAX}= 5.0, E_{FMIN}= -5.0

[c] PSS constants: K_{STAB}= 20, T_w= 1.4 sec
T_1= 0.154 sec, T_2= 0.033 sec
V_{SMAX}= 0.2, V_{SMIN}= -0.2

LIST OF PUBLICATIONS

[**1**] Kamalesh Chandra Rout, P.C. Panda, ”Improvement of dynamic stability of a single machine infinite bus power system using fuzzy logic based power system stabilizer”, International Conference on Electrical Power and Energy Systems (ICEPES - 2010), Aug 26 - 28, 2010, NIT Bhopal.

[**2**] Kamalesh Chandra Rout, P.C. Panda, ”Power system dynamic stability enhancement of SMIB using fuzzy logic based power system stabilizer”, International Conference on Advances in Power Electronics and Instrumentation Engineering (PEIE - 2010) Sep 07 - 08, 2010, Kochi, Kerala.

[**3**] Kamalesh Chandra Rout, P.C. Panda, ”An adaptive fuzzy logic based power system stabilizer for enhancement of power system stability”, IEEE International Conference on Industrial Electronics, Control and Robotics (IECR - 2010), Dec 27 - 30, 2010 NIT Rourkela.

[**4**] Kamalesh Chandra Rout, P.C. Panda, ”Performance analysis of power system dynamic stability using fuzzy logic based PSS for positive and negative value of K5 constant”, IEEE International Conference on Computer, Communication and Electrical Technology (ICCCET - 2011), March 18 - 19, 2011, NCE, Tirunelvelli.

AUTHOR'S BIOGRAPHY

Kamalesh Chandra Rout was born to Sri Kailash Chandra Rout and Smt. Promodini Rout on 26th June, 1981 at Dhenkanal, Odisha, India. He obtained a Bachelors degree in Electrical Engineering from University College of Engineering (U.C.E), Burla, Odisha in 2004. He joined the Department of Electrical Engineering, National Institute of Technology, Rourkela in January 2009 as an Institute Research Scholar to pursue M.Tech by Research.